CORRECTION

Insulin signaling promotes germline proliferation in *C. elegans*

David Michaelson, Dorota Z. Korta, Yossi Capua and E. Jane Albert Hubbard

There were errors published in *Development* **137**, 671-680.

We recently discovered that the genotypes of several strains that we reported as *daf-16(mu86)* actually carry the *daf-16(m26)* allele. Correct genotypes for strains listed in Tables S1 and S3 and those used in experiments reported in Fig. 3C and Fig. S2C and related text and legends are:

DR1309: *daf-16(m26); daf-2(e1370)*
GC967: *daf-16(m26); glp-1(ar202); naEx148 [pGP30(DAF-16::GFP) + sur-5::GFP]*
GC1109: *daf-16(m26); daf-2(e1370); naEx202[pGC461 (Plag-2::daf-16::GFP) + pRF4]*
GC1112: *daf-16(m26); daf-2(e1370); naEx148[pGP30 (daf-16::GFP) + sur-5::GFP]*
GC1144: *daf-16(m26);daf-2(e1370); naIs43[pGC492(Prpl-11.1::daf-16cDNA::GFP::nos2 3'UTR unc-119(+))]*. Note that the legend to Table S1 indicates that expression of the *daf-16::GFP* transgene in GC1144 was silenced subsequent to data collection.

The conclusions of the paper are not altered by these errors. The authors apologise to readers for these mistakes.

Development 137, 671-680 (2010) doi:10.1242/dev.042523

Insulin signaling promotes germline proliferation in *C. elegans*

David Michaelson, Dorota Z. Korta, Yossi Capua and E. Jane Albert Hubbard*

SUMMARY

Cell proliferation must be coordinated with cell fate specification during development, yet interactions among pathways that control these two critical aspects of development are not well understood. The coordination of cell fate specification and proliferation is particularly crucial during early germline development, when it impacts the establishment of stem/progenitor cell populations and ultimately the production of gametes. In *C. elegans*, insulin/IGF-like receptor (IIR) signaling has been implicated in fertility, but the basis for the fertility defect had not been previously characterized. We found that IIR signaling is required for robust larval germline proliferation, separate from its well-characterized role in preventing dauer entry. IIR signaling stimulates the larval germline cell cycle. This activity is distinct from Notch signaling, occurs in a predominantly germline-autonomous manner, and responds to somatic activity of *ins-3* and *ins-33*, genes that encode putative insulin-like ligands. IIR signaling in this role acts through the canonical PI3K pathway, inhibiting DAF-16/FOXO. However, signaling from these ligands does not inhibit *daf-16* in neurons nor in the intestine, two tissues previously implicated in other IIR roles. Our data are consistent with a model in which: (1) under replete reproductive conditions, the larval germline responds to insulin signaling to ensure robust germline proliferation that builds up the germline stem cell population; and (2) distinct insulin-like ligands contribute to different phenotypes by acting on IIR signaling in different tissues.

KEY WORDS: Cell cycle, Notch, Dauer, *ins-3*, *ins-33*, *C. elegans*

INTRODUCTION

Development of multicellular organisms requires the coordination of cell proliferation and specification. Although major cell cycle regulators are defined, less is known about the control of cell proliferation by growth factors within developmental contexts (e.g. Edgar and Lehner, 1996; Fichelson et al., 2005; Orford and Scadden, 2008). Furthermore, the control of proliferation within stem and transit amplifying cell populations is not well understood (Kohlmaier and Edgar, 2008). The intersection of cell proliferation and cell fate specification is important for understanding human diseases, particularly cancer, which is characterized by the dysregulation of both proliferation and fate (see Hanahan and Weinberg, 2000; Sancho et al., 2004).

The insulin/IGF receptor (IIR) family is conserved across metazoans and controls multiple aspects of cell growth and metabolism (Taguchi and White, 2008). Defects in IIR-associated pathways account for a host of human diseases, including diabetes and cancer. Invertebrate model organisms have contributed much towards understanding IIR signaling on the cellular and organismal levels, especially with respect to metabolism, developmental decisions and lifespan. The *C. elegans* genome contains one IIR-encoding gene *daf-2* (Kimura et al., 1997), and 40 putative insulin-like peptide genes (Pierce et al., 2001). The IIR signaling cascade initiated by DAF-2 is highly conserved from *C. elegans* to mammals: receptor activation signals through a PI 3-kinase cascade that results in phosphorylation and nuclear exclusion of a FOXO transcription factor (*C. elegans* DAF-16).

Developmental Genetics Program, Helen and Martin Kimmel Center for Stem Cell Biology, Skirball Institute of Biomolecular Medicine, Department of Pathology, New York University School of Medicine, 540 First Avenue, New York, NY 10016, USA.

*Author for correspondence (jane.hubbard@med.nyu.edu)

Accepted 21 December 2009

C. elegans daf-2 is implicated in many genetically separable processes, including the dauer decision, lifespan control, and reproductive timing (see Baumeister et al., 2006; Fielenbach and Antebi, 2008; Gami and Wolkow, 2006; Hu, 2007; Li and Kim, 2008; Murphy, 2006). Mutants with reduced *daf-2* activity enter dauer even under replete conditions, and have extended lifespan and reproductive timing (Gottlieb and Ruvkun, 1994; Kenyon et al., 1993; Larsen et al., 1995; Vowels and Thomas, 1992).

C. elegans germline development (Hirsh et al., 1976), like that of many animals, includes a phase in which undifferentiated germ cells proliferate extensively, forming a stem cell or progenitor pool that maintains gamete production throughout reproductive adulthood. In *C. elegans*, the GLP-1/Notch receptor pathway maintains germ cells in the undifferentiated (mitotic) state and/or prevents their differentiation (meiotic entry) (Austin and Kimble, 1987). Two DSL family ligands, LAG-2 and APX-1 are expressed in the distal tip cell (DTC) (Henderson et al., 1994; Nadarajan et al., 2009), and activate GLP-1 in neighboring germ cells. Loss of Notch signaling causes all germ cells to differentiate (enter meiosis), whereas constitutive Notch signaling prevents differentiation (Austin and Kimble, 1987; Berry et al., 1997). The *C. elegans* germ line is, therefore, a prototypical system in which signaling promotes the undifferentiated (proliferative) versus differentiated (non-proliferative) fate. In such systems, the relative contributions of signaling to mitotic cell fate specification and cell cycle control can be difficult to parse.

Independently of cell fate patterning by Notch pathway activity, the gonadal sheath regulates larval germline proliferation (Killian and Hubbard, 2005; McCarter et al., 1997). Therefore, other signaling contributes to the control of robust germline proliferation.

In this study, we uncover a novel role for DAF-2 in germline development. We find that IIR signaling promotes robust germline cell cycle progression during the crucial larval expansion phase. We demonstrate that IIR activity affects cell cycle kinetics in a manner

distinct from that of Notch signaling, is separate from the dauer decision, does not account for the sheath signal, and occurs through the canonical IIR-PI3K-FOXO pathway primarily in the germ line. We further implicate somatic activity of two of the 40 putative insulin-like peptide ligands in this function.

MATERIALS AND METHODS

Strains and plasmids

Strains (see Table S1 in the supplementary material) were derived from N2 wild type (Bristol) and handled using standard methods (Brenner, 1974). Plasmids used are listed in Table S2 in the supplementary material.

Apoptosis

A procedure modified from Gumienny et al. was used (Gumienny et al., 1999): worms were washed in M9, incubated in 200 μl of 33 mM SYTO12 (Invitrogen) in M9 for 5 hours at room temperature in the dark, destained for 1 hour in the dark on a fresh plate of OP50, and scored live while paralyzed in levamisole.

RNAi

RNAi by bacterial feeding was performed as described by Timmons et al. (Timmons et al., 2001). Unless otherwise indicated, parental worms were grown on OP50 at 15°C, their progeny were synchronized by L1 hatch-off (Pepper et al., 2003) and grown at 20°C to the desired stage. Bacteria bearing the empty RNAi expression vector L4440 served as a negative control.

Microscopy

Images were collected from a Zeiss Imager Z1 with an Apotome Axioimager (Carl Zeiss) using an AxioCamMRm digital camera and Zeiss AxioVision and NIH ImageJ software.

Time-course analysis

After synchronization by L1 hatch-off, vulval development was used as the primary developmental stage marker [see figure 4 of Seydoux et al. (Seydoux et al., 1993)]. Early L3 is characterized by an undivided P6p under a distinct anchor cell; L3/L4 by vulval morphology and initiation of the gonad turn. 'Early adult' stage was 8-10 hours post-mid to mid/late L4 at 20°C, and characterized by adult vulval morphology but few if any embryos in the uterus.

Determination of number of nuclei in the proliferative zone, distance to transition zone, and mitotic index

The 'number of nuclei in the proliferative zone' included all the germ nuclei between the distal tip and the transition zone, as determined after ethanol fixation and DAPI staining (Pepper et al., 2003). The distal edge of the transition zone border was defined as the first cell diameter in which two or more nuclei displayed the characteristic crescent shape (Crittenden et al., 2006). 'Distance to transition zone' was measured in cell diameters from the distal tip to the transition zone border. The mitotic index is the number of metaphase and anaphase figures over the total number of nuclei in the proliferative zone (Maciejowski et al., 2006).

5-ethynyl-2′-deoxyuridine (EdU) labeling

EdU-labeled bacteria were fed to L4 N2 and *daf-2(e1370)* worms for 30 minutes prior to fixation, and processed as described by Dorsett et al. (Dorsett et al., 2009), with the following modifications. Whole worms or dissected gonads (both yielded similar results) were fixed for 10 minutes in 3.7% paraformaldehyde (Electron Microscopy Sciences) in PBST, washed in PBST, incubated for 5 minutes in –20°C methanol, and washed three times in PBST. After the Click-IT EdU reaction (Molecular Probes), preparations were imaged. S-phase index is the percentage of the DAPI-labeled proliferative zone nuclei that are EdU positive. Nuclei with any EdU labeling (individual chromosomes or all chromosomes) were scored as positive.

Quantification of DNA content

The relative DNA content of proliferative zone nuclei was determined as described (Feng et al., 1999), with the following modifications. Worms were grown on OP50 at 20°C to the mid to mid/late L4 stage, ethanol fixed for 10 minutes, incubated for 1 hour at 37°C with 40 μg/ml RNAse A in PBS, then imaged on agar pads in propidium iodide (Vector Laboratories, H-1300). The area and average intensity was determined for each nucleus in each *z*-layer (0.5 μm intervals) using ImageJ. The sum of the products of area × the average intensity for each layer gave the total fluorescence per nucleus. Average background intensity (from four similarly sized circles within or adjacent to gonad) was subtracted from measurements of each slice. 2N DNA content was established from non-mitotic somatic cells of the vulva and uterus in the same animal and from sets of daughter chromosomes of anaphase germ nuclei, and was verified using 4N nuclei (metaphase figures and pachytene nuclei). To obtain the haploid equivalent, the total fluorescence from each germ cell nucleus was divided by one half of the 2N value obtained from the somatic cells. Every nucleus was measured from the distal tip to the first cell diameter within four cell diameters of the transition zone (to avoid meiotic S).

Cell ablations

Parental GC678 *tnIs6[lim-7::GFP];qIs19[lag-2::GFP]* worms were grown on OP50 at 20°C; their progeny were synchronized by L1 hatch-off, washed and placed on plates with *daf-16(RNAi)*-inducing or L4440-bearing bacteria (empty RNAi expression vector, used as a negative control), and grown at 20°C until the early L3 stage. Laser microsurgery (Photonics Instruments Micropoint Laser System) of both SS cells in a single gonad arm was carried out as described (Killian and Hubbard, 2005). Unablated controls were the unoperated gonad arm and additional siblings mounted on the same slides as operated animals. Ablated worms were placed back onto *daf-16(RNAi)* or L4440 and allowed to develop until adulthood at 20°C. Adult gonad arms with a GFP-positive DTC but no GFP-positive cells at the normal sheath location were considered to be successful ablations. To control for *daf-16* RNAi efficacy, the same bacterial cultures were tested for suppression of *daf-2(e1370)* dauer at 25°C by L1 feeding.

Reproductive timing and brood size

Experiments were performed as described (Dillin et al., 2002). Synchronized populations of L1 (1 hour post-hatch) *daf-2 (e1370)*, *ins-3(ok2488)* and *ins-33(tm2988)* worms were grown on *daf-16(RNAi)* and L4440 until the mid to mid/late L4 stage at 20°C. Individual worms were placed on separate plates at 20°C, transferred to new plates every 12 hours, and live progeny counted.

DAF-16::GFP nuclear localization and expression of *sod-3::GFP*

Worms (GC865 and CF1553) were grown on RNAi bacteria targeting *daf-2*, *ins-3* or *ins-33* (or L4440) to the mid to mid/late L4, and images captured. All animals were examined within 10 minutes because, after 15 minutes on the agar pad (in 0.4 mM levamisole to immobilize worms), DAF-16::GFP translocated to the nucleus even in controls.

RESULTS

IIR signaling is required for the proper accumulation of undifferentiated germ cells

Several mutations in *daf-2*, the gene encoding the *C. elegans* insulin/IGF-like receptor (IIR), cause a sterile or a reduced-fecundity adult phenotype, suggesting a role for IIR signaling in gonadogenesis or germline development (Gems et al., 1998; Malone and Thomas, 1994; Patel et al., 2008; Tissenbaum and Ruvkun, 1998). We examined a well-characterized temperature-sensitive, dauer-constitutive allele, *daf-2(e1370)*, under non-dauer-inducing conditions (well fed and at a semi-permissive temperature of 20°C). Compared with stage-matched wild-type (N2) animals, we found that *daf-2(e1370)* adult hermaphrodites and males have fewer germ cells in the distal proliferative zone (Fig. 1; see also Table S3 in the supplementary material). This region contains pre-meiotic stem or progenitor germ cells, the majority of which are in the mitotic cell cycle (Crittenden et al., 2006).

To further characterize the *daf-2* germline phenotype, we conducted temperature-shift and time-course analyses (Fig. 1A). We observed severely reduced numbers of distal germ cells after a shift to the non-permissive temperature early in the third larval stage (L3; after the dauer entry decision). This shift reduced the average brood

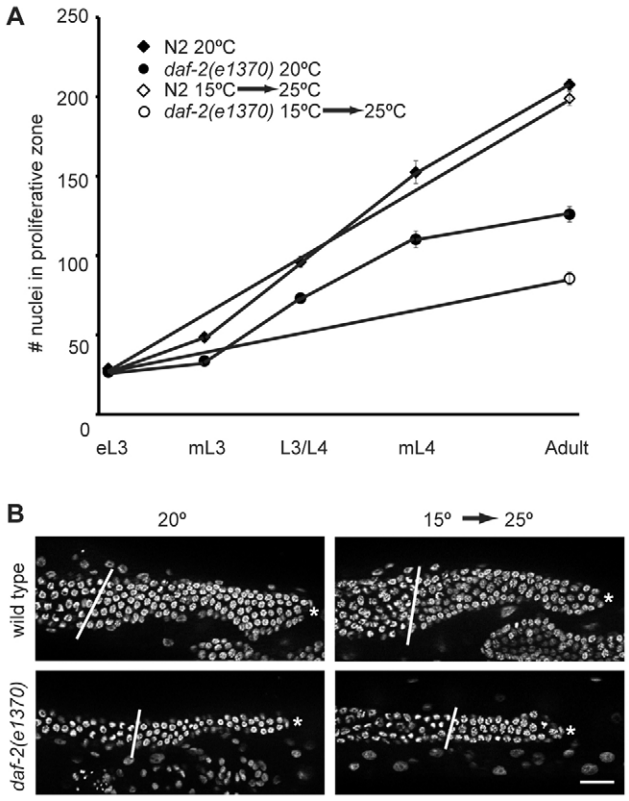

Fig. 1. Insulin receptor activity is required for robust larval germline proliferation. (**A**) Total number of nuclei in the proliferative zone in wild-type (N2; black diamonds) and *daf-2(e1370)* (black circles), and in temperature-shifted N2 (white diamonds) and *daf-2(e1370)* (white circles). Error bars indicate s.e.m. (**B**) Representative DAPI-stained germ line of early adult N2 and *daf-2(1370)*. Left, 20°C; right, shift from 15°C to 25°C at early L3. White line indicates the transition zone border; asterisk, the distal end. Scale bar: 20 μm.

size to 17±1.9 progeny (n=10 broods; wild-type control broods averaged >200), underscoring the importance of robust larval proliferation for fecundity. These results also suggest that the germline and dauer phenotypes are separable.

Time-course analysis at 20°C (<1% dauer; see Table S4A in the supplementary material) revealed a defect in the amplification of proliferative zone germ cell numbers during the L3 and L4 stages. After the early L3 stage, the proliferative zone of *daf-2(e1370)* animals contained, on average, fewer germ cells than that of stage-matched N2 animals (Fig. 1A). The difference was first evident in the mid-L3 but became more pronounced at later stages, consistent with a cumulative effect. We found a similar but less-marked defect in germ cell numbers after L1-initiated *daf-2(RNAi)* feeding (see Table S3 in the supplementary material; see also Fig. 3B; at 27°C, the same RNAi yields 100% dauer; see Table S4C in the supplementary material).

In other systems, insulin/IGF signaling is associated with cell size control (Edgar, 2006). We measured cell volume in 40-50 total germ cells from multiple individuals. RNAi directed against *daf-2*, *ins-3* or *ins-33* (see below) had no effect on L4 germ cell volume, nor did a *daf-2* mutation (see Table S5 in the supplementary material).

Notch and IIR pathways influence germline proliferation by different cellular mechanisms

A reduction in the number of cells in the proliferative zone could result from elevated cell death, a change in the balance between proliferation and differentiation, and/or a cell-cycle defect within the proliferative zone. We examined each of these possibilities. We stained late-L4 and young adult *daf-2* mutants with SYTO-12 to mark apoptotic nuclei, and found that although all animals contained SYTO-12-positive cells in the loop region, as expected (Gumienny et al., 1999), none contained SYTO-12-positive cells in the distal germ line (n>80 each stage; data not shown). Therefore, inappropriate distal zone apoptosis does not account for the phenotype.

The distance from the distal tip to the transition zone is a measure of the effective 'reach' of the DTC signal to deter meiotic entry, and it often correlates well with cell numbers (e.g. Eckmann et al., 2004). We examined this parameter in multiple reduction-of-function (rf) *glp-1* and *daf-2* mutants at the L4 stage. Consistent with previous observations (Hansen et al., 2004), the distance from the distal tip to the transition zone in *glp-1(rf)* mutants raised at a semi-permissive temperature was considerably reduced relative to that measured in wild type (12-13 cell diameters in the mutant versus 23 in wild type; Fig. 2A,C). By contrast, the distance to transition was only slightly reduced in three different *daf-2(rf)* alleles (19-21 cell diameters versus 23; Fig. 2A,C). The effects of both the *glp-1* and the *daf-2* mutations were statistically significant, so a minor role for *daf-2* in preventing differentiation cannot be ruled out. However, the effect of *daf-2* was much smaller than that of *glp-1*. These data also suggest that cell number and distance to transition do not always correlate well.

To determine whether the frequency of germ cell divisions was altered in *daf-2(rf)* and *glp-1(rf)* mutants, we measured the mitotic index. The germline mitotic index in *daf-2* mutant larvae (but not in adult, data not shown) was reduced relative to that of wild type (Fig. 2B), consistent with our time-course analysis and with previous work (Pinkston et al., 2006). In striking contrast, the mitotic index of *glp-1(rf)* mutant larvae was not reduced relative to that of wild type (Fig. 2B,C). These results support the hypothesis that DAF-2/IIR signaling through DAF-16 primarily affects the cell cycle, whereas GLP-1/Notch signaling affects the mitosis/meiosis decision, rather than accelerating the larval germline cell cycle rate per se. If the effects of *glp-1*/Notch and *daf-2*/IIR on larval germline proliferation were indeed largely independent, reducing both should cause both phenotypes. Indeed, *daf-2(e1370) glp-1(e2141)* double mutants raised at a semi-permissive temperature for both alleles exhibited both the mitotic index and the meiotic entry defects, with no indication of synergy (Fig. 2A-C).

We further explored the effects of *daf-2* on the cell cycle by examining S-phase index and DNA content. We compared the number of proliferative zone nuclei in S-phase in L4 wild-type and *daf-2(e1370)* worms. Although more than 50% of the nuclei labeled with EdU in both strains, the proportion of EdU-labeled nuclei was significantly lower in *daf-2(e1370)* worms compared with wild type (Fig. 2D; see also Fig. S1C in the supplementary material). We then examined the effects of *daf-2(e1370)* on the L4 germline cell cycle using a propidium iodide-based protocol (Fig. 2E). We observed a shift to higher haploid equivalents in germlines of *daf-2* larvae relative to those of N2. In particular, the number of nuclei ~2N was reduced, whereas the number ~4N was elevated.

Taken together, several conclusions can be drawn from the results of the M and S phase indices and DNA content measurements. A decrease in both M and S phase indices suggests that the cells are cycling less frequently. Furthermore, because we see a reduction in

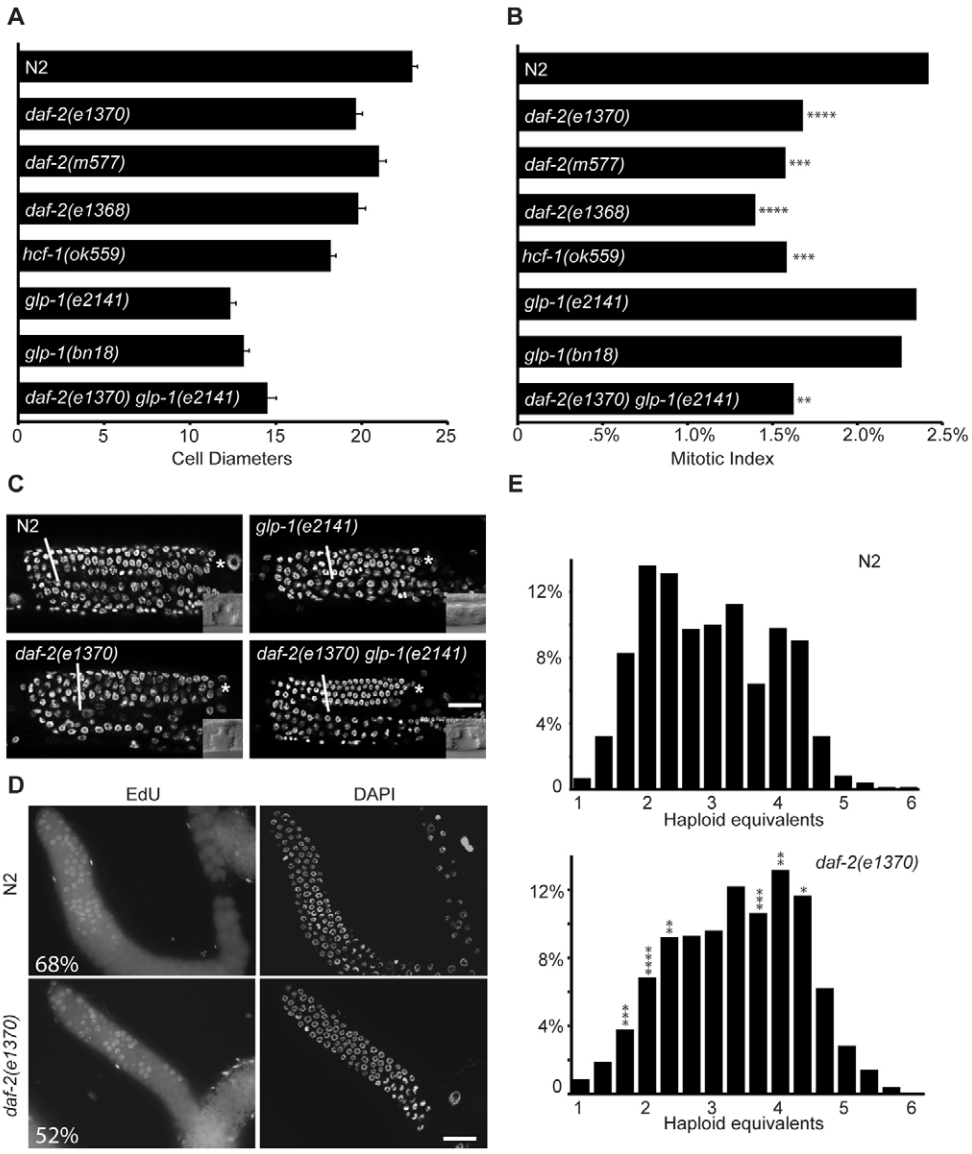

Fig. 2. Insulin signaling primarily affects cell cycle. (**A**) The distance in cell diameters from the distal tip to the transition zone in L4 N2 worms, *daf-2*, *hcf-1* and *glp-1* mutants. Error bars indicate s.e.m.; $P<0.001$, two-tailed Student's *t*-test versus N2 control. (**B**) Mitotic index in the same individuals as in A. The number of gonad arms and number of nuclei for both A and B is: N2, 53 and 8144; *daf-2(e1370)*, 54 and 6373; *daf-2(m577)*, 25 and 3235; *daf-2(e1368)*, 25 and 3146; *hcf-1(ok559)*, 36 and 3789; *glp-1(e2141)*, 40 and 2641; *glp-1(bn18)*, 38 and 2743; *daf-2(e1370) glp-1(e2141)*, 35 and 2832. $^{**}P<0.01$; $^{***}P<0.001$; $^{****}P<0.0001$; otherwise $P>0.1$; two-tailed Mann-Whitney *U*-test versus N2 control. (**C**) Representative DAPI-stained mid- to mid/late-L4 worms grown as in A, B. Insets show vulvae from the same individual worms in each panel. (**D**) EdU labeling of S-phase nuclei. The number of gonad arms and number of nuclei is: N2, 26 and 3996; and *daf-2(e1370)*, 25 and 3419. $P<0.0001$, two-tailed Mann-Whitney U-test. See Fig. S1 in the supplementary material for box plots of data in A, C and D. Labels and scale in C and D are as in Fig. 1B. (**E**) Quantification of DNA content in N2 and *daf-2(e1370)* L4 larvae. The number of gonad arms and number of nuclei is: N2, 15 and 1448; and *daf-2(e1370)*, 15 and 1270. $^{*}P<0.05$; $^{**}P<0.01$; $^{***}P<0.001$; $^{****}P<0.0001$; otherwise $P>0.05$; two-tailed Mann-Whitney U-test versus N2 control.

the number of nuclei with ~2N DNA content and a concomitant elevation in the number of nuclei with a ~4N DNA content, we conclude that the delay is in G2.

The PI3K branch of the IIR signaling pathway mediates the *daf-2* role in germline proliferation

To determine whether the conserved PI3K branch of the DAF-2 signaling pathway promotes larval germ cell proliferation, we examined epistasis relationships (Gil et al., 1999; Lin et al., 1997; Ogg et al., 1997; Ogg and Ruvkun, 1998; Rouault et al., 1999). If this pathway is responsible for the *daf-2* germline phenotypes, reducing the activity of DAF-18/PTEN or DAF-16/FOXO should ameliorate the effect of reduced *daf-2*. We counted the number of adult proliferative zone germ cells in mutant/RNAi treatments that reduced the activity of both *daf-2* and *daf-18* or *daf-16* (that is, *daf-18* or *daf-16* RNAi in the *daf-2* mutant, *daf-2* RNAi in the *daf-18* or *daf-16* mutants, or double mutants). In each case, reducing *daf-18* or *daf-16* restored normal germ cell numbers (Fig. 3A,B; see Table S3 in the supplementary material). Thus, the canonical pathway mediates the role of *daf-2* in larval germline proliferation.

We then sought to determine whether the *daf-2* pathway acts in the germ line or the soma to influence germline proliferation. Previous mosaic analysis indicated that for many phenotypes *daf-2* acts cell non-autonomously, but with a possible germline-autonomous component for fertility (Apfeld and Kenyon, 1998). We first examined data from microarray studies in early embryos (Hill et al., 2000), and found that many DAF-2 pathway components (including *akt-1*, *daf-18* and *daf-16*) are germline transcribed, as is *hcf-1*, a constitutively nuclear co-factor that inhibits DAF-16 largely independently of the insulin pathway (Li et al., 2008). Consistent with a *daf-16*-dependent positive role for HCF-1 in germline proliferation, *hcf-1* mutants have a defect similar to that of *daf-2* mutants (Fig. 2A,B; see also Table S3 in the supplementary material; Fig. 3B).

To investigate further the germline versus soma activity of pathway components, we tested the efficacy of RNAi knockdown of several pathway components in the *rrf-1* mutant background that reduces RNAi effectiveness in the soma but retains it the germ line [*rrf-1(pk1417)* (Sijen et al., 2001)]. RNAi directed against genes encoding both positively and negatively acting components of the pathway,

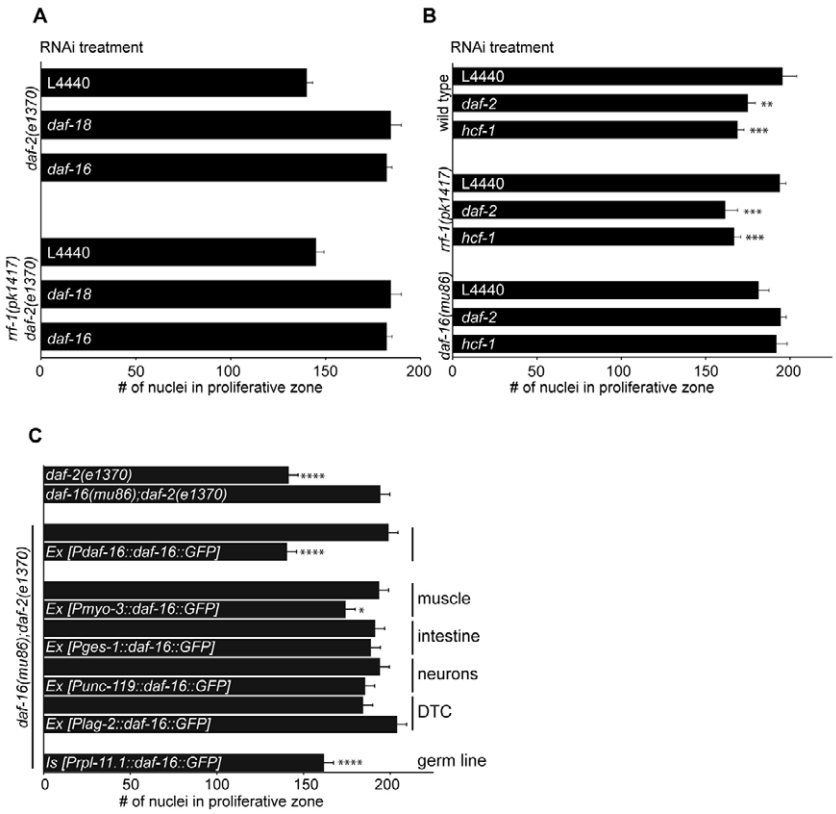

Fig. 3. DAF-2 signaling pathway components act in the germ line for robust larval germline proliferation. (**A**) Number of nuclei in proliferative zone of early adult *daf-2(e1370)* and *rrf-1(pk1417);daf-2(e1370)* worms treated with RNAi targeting *daf-18* or *daf-16*. Error bars indicate s.e.m.; $P<0.0001$, two-tailed Student's *t*-test versus appropriate L4440 negative control. (**B**) Number of nuclei in proliferative zone of early adult N2, *rrf-1(pk1417)* and *daf-16(mu86)* worms treated with RNAi targeting *daf-2* or *hcf-1*. Error bars indicate s.e.m. Statistics: $^{**}P<0.01$; $^{***}P<0.001$; otherwise $P>0.1$; two-tailed Student's *t*-test versus appropriate L4440 control. (**C**) Number of nuclei in proliferative zone of early adult worms in indicated genotypes. 'Ex' genotypes express the DAF-16::GFP fusion driven by the indicated promoter and non-array-bearing siblings are shown as comparisons (sibling pairs are indicated by vertical lines). Tissue-specific activity of the promoters is indicated; the *lag-2* promoter is not exclusive to the DTC. For the *rpl-11.1* promoter ('Is' genotype) the *daf-16(mu86);daf-2(e1370)* double mutant background strain is shown for comparison. Note, expression of DAF-16::GFP in GC1144 *nals43[Prpl-11.1::DAF-16::GFP]* has since been silenced in this line (see Table S1 in the supplementary material for details). Error bars indicate s.e.m. $^{*}P<0.05$; $^{****}P<0.0001$; otherwise, $P>0.1$. Top pair, two-tailed Student's *t*-test versus *daf-16*, *daf-2*; all others, one-tailed Student's *t*-test versus siblings. See Fig. S2 in the supplementary material for corresponding box plots.

from *daf-2* to *daf-16*, remains effective in the *rrf-1* mutant (Fig. 3A,B; see also Table S3 in the supplementary material), suggesting that these components act in the germ line.

To confirm a germline requirement for DAF-16, we took two additional approaches: mosaic analysis and tissue-specific gene expression, using *daf-16(mu86)* suppression of the *daf-2(e1370)* germline proliferation defect as a read-out (Fig. 2C). Simple transgenic arrays are not normally expressed in the germ line (Kelly et al., 1997), but we found that two independent transgenic arrays, *muEx108* (Lin et al., 2001) and *naEx148* [based on Henderson and Johnson (Henderson and Johnson, 2001)], expressed DAF-16::GFP in the germ line (see Fig. S3 in the supplementary material) and reversed the *daf-16(–)* suppression of the *daf-2* germline defect (Fig. 3C; see also Table S3 in the supplementary material), although GFP was not visible in the germ line. We speculate that only low levels of DAF-16 are required to rescue the germline phenotype, and that these are insufficient to visualize GFP. We then used the *daf-16(mu86);daf-2(e1370); muEx108[daf-16(+)]* strain for a simple germline/soma mosaic analysis (see Table S8 in the supplementary material). Briefly, we shifted individual animals of the genotype *daf-16;daf-2;Ex[daf-16::GFP]* and determined (1) the brood size and (2) whether the transgene passed through the germ line to the progeny. The results are consistent with a germline requirement for *daf-16*, but also indicate a possible somatic requirement. Specifically, 97% (475/487) of worms that transmitted the array to their progeny had small broods (equivalent to those of the *daf-2(e1370)* single mutant). Conversely, of those that failed to transmit the array, 74% (17/23) had brood sizes comparable to those of the *daf-16;daf-2* double mutant. Therefore, loss of *daf-16(+)* from the germ line correlates with a considerable restoration of fecundity in *daf-2(e1370)*.

Finally, we assayed DAF-16::GFP expression from heterologous promoters. Neuronal and intestinal DAF-16 expression largely reverses *daf-16* mutant suppression of the *daf-2* dauer and lifespan phenotypes, respectively (Libina et al., 2003) (see Table S4B in the supplementary material). Expression of DAF-16::GFP in neurons, intestine, or the DTC, did not reverse *daf-16(–)* suppression of the *daf-2* germline defect, while expression from the *myo-3* promoter (muscle/proximal sheath) somewhat reduced the number of proliferative germ cells (Fig. 3C; see Table S3 in the supplementary material), suggesting a minor contribution from *myo-3*-expressing tissues to germline proliferation (see also Table S8 in the supplementary material). Importantly, the number of proliferative germ cells was even lower upon germline-specific DAF-16::GFP expression (*Prpl-11.1*; Fig. 3C; see also Table S3 in the supplementary material) and was comparable to that in the *daf-2* single mutant.

Taken together, our studies are consistent with a primary germline requirement for *daf-2*, *daf-16*, *daf-18* and *hcf-1* in controlling germline proliferation, with a possible additional minor contribution from the soma.

Proper larval accumulation of proliferative germ cells requires *ins-3* and *ins-33* in the soma

To determine which of the 40 putative insulin-like ligands (Li et al., 2003; Pierce et al., 2001) promote larval germline proliferation, we used a genetic assay based on the observation that a reduction of robust larval germline proliferation can enhance the penetrance of proximal germline tumor formation (Pro phenotype) in *glp-1*(Pro) mutants (Killian and Hubbard, 2004; Killian and Hubbard, 2005; McGovern et al., 2009) (see legend to Fig. S4 in the supplementary material for additional explanation). The Pro phenotype of two *glp-1(Pro)* mutants (*ar202* and *ar218*) was enhanced by *daf-2(e1370)* (data not shown). We individually targeted each of the 40 predicted

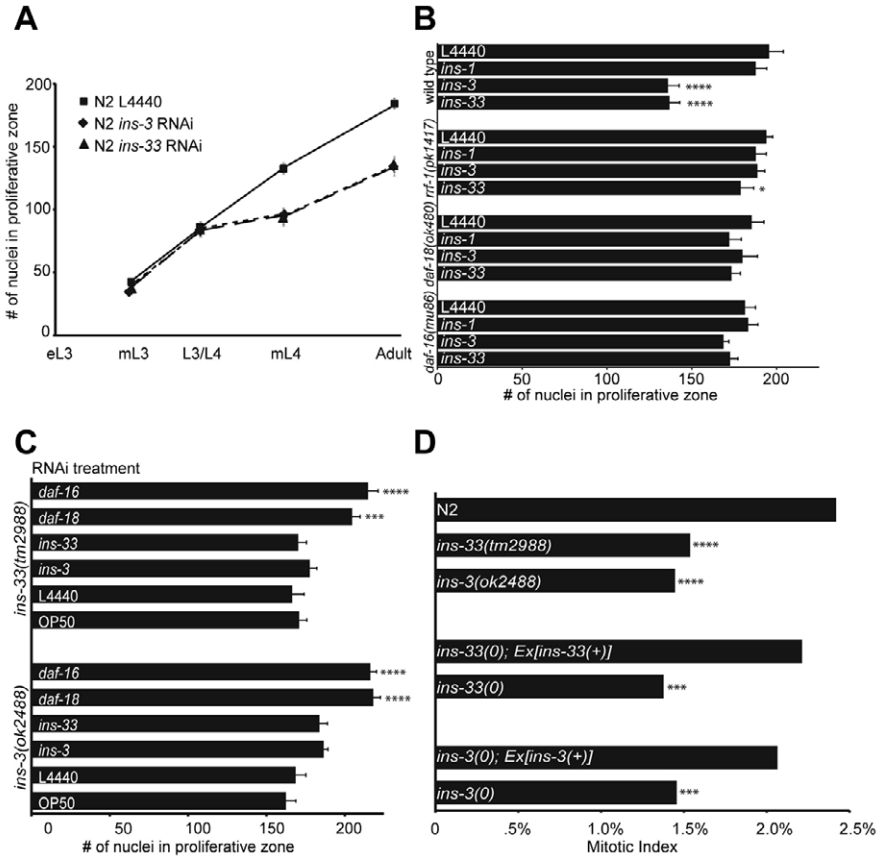

Fig. 4. *ins-3* and *ins-33* are required in the soma and depend on *daf-18* and *daf-16* to promote robust larval germline proliferation. (**A**) Number of proliferative zone nuclei in germ lines of adult N2 worms raised from hatching on bacteria carrying L4440 (black line and squares) or RNAi targeting *ins-3* (dashed line, diamonds) or *ins-33* (dotted line, triangles). Error bars indicate s.e.m. (**B**) Number of proliferative zone nuclei in germ lines of early adult N2, *rrf-1(pk1417)*, *daf-18(ok480)* and *daf-16(mu86)* worms grown from hatching on L4440 or RNAi targeting *ins-1* (negative control), *ins-3* or *ins-33*. Error bars indicate s.e.m. Statistics: *P<0.05; ****P<0.0001; unmarked, P>0.05; two-tailed Student's *t*-test versus appropriate L4440 control. (**C**) Number of proliferative zone nuclei in germ lines of early adult *ins-3* or *ins-33* mutants on indicated RNAi. Error bars indicate s.e.m. ***P<0.001; ****P<0.0001; unmarked, P>0.05 except *ins-3(RNAi)* in *ins-3(tm2488)* (P=0.02); two-tailed Student's *t*-test versus appropriate L4440 control. (**D**) The L4 mitotic index in the same strains as in C, and in these strains carrying extrachromosomal arrays containing *ins-3(+)* or *ins-33(+)*. Siblings that had lost the array (non-Rol) are indicated as *ins-3(0)* and *ins-33(0)*, respectively. '*Ex[ins-33(+)]*' and '*Ex[ins-3(+)]*' refer to *naEx197* and *naEx187*, respectively. Similar results were obtained from *naEx186* and *naEx195* (see Table S3 in the supplementary material). The number of gonad arms and number of nuclei is: N2, 53 and 8144; *ins-33(tm2988)*, 38 and 5138; *ins-3(ok2488)*, 40 and 4840; *ins-33(tm2988)* with *naEx187*, 25 and 3728, and siblings, 25 and 3364; *ins-3(ok2488)* with *naEx197*, 25 and 3704, and siblings, 25 and 3339. ***P<0.001; ****P<0.0001; Mann-Whitney U-test (two-tailed for mutants versus N2; one-tailed for sibling pairs). P>0.1 for Ex strains versus N2. See Fig. S5 in the supplementary material for box plots corresponding to B, C and D.

insulin genes by RNAi feeding and tested them for enhancement of the *glp-1(ar202)* Pro phenotype. Out of the 40 genes tested, two putative ligands, *ins-3* and *ins-33*, enhanced the *glp-1(ar202)* mutant phenotype (see Fig. S4 in the supplementary material).

Further investigation substantiated the role of *ins-3* and *ins-33* in larval germline proliferation. Treatment with *ins-3* or *ins-33* RNAi significantly reduced the number of proliferative zone germ cells compared with L4440 or *ins-1* RNAi negative controls in both males and hermaphrodites (Fig. 4; see also Table S3 in the supplementary material). Interestingly, RNAi targeting either *ins-3* or *ins-33* mRNA gave nearly identical results at all developmental stages, suggesting that they act together or in series to promote robust larval germline proliferation. Time-course analysis indicated that *ins-3* or *ins-33* RNAi defects (Fig. 1A, Fig. 4A) were less severe than those of *daf-2* mutants shifted to the restrictive temperature, suggesting that additional redundantly-acting ligands might contribute. Results of timed shifts to and from RNAi bacteria indicate a requirement for *ins-3* and *ins-33* after the mid-L3 stage (see Table S7 in the supplementary material), consistent with that of *daf-2*. RNAi targeting *ins-3* and *ins-33* in *rrf-1(pk1417)* resulted in near-normal germline proliferation, suggesting that *ins-3(+)* and *ins-33(+)* are required in the soma (Fig. 4B). The canonical IIR pathway acts downstream of *ins-3* and *ins-33*, as the phenotype was suppressed in *daf-18* and *daf-16* mutant backgrounds (Fig. 4B).

Deletion mutant alleles of *ins-3* and *ins-33* cause defects similar to those caused by RNAi with respect to enhancement of the *glp-1(ar202)* Pro phenotype and reduction of germ cell numbers (see Tables S3, S6 in the supplementary material). Their effects on germ cell number and mitotic index were *daf-18* and *daf-16* dependent (Fig. 4C). Reintroducing *ins-3(+)* and *ins-33(+)* into the respective mutant strains on simple transgenic arrays rescued these defects (see Table S3 in the supplementary material; Fig. 4D), verifying that the mutant phenotype is due to the deletion of these genes. Overexpression of *ins-3* or *ins-33* did not elevate the number of proliferative germ cells,

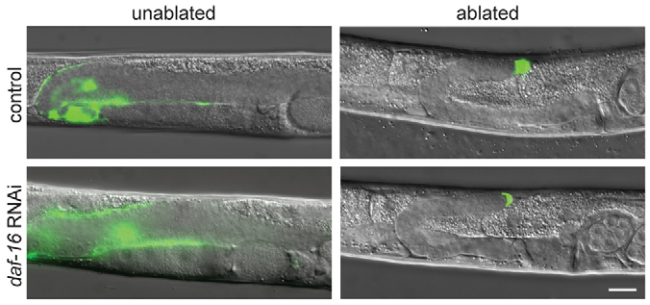

Fig. 5. *daf-16* is not required for the regulation of germline proliferation by the somatic gonadal sheath. Representative unablated control (left) and 2SS-cell ablated (right) gonad arms of GC678 *tnIs6[Plim-7::GFP];qIs19[Plag-2::GFP]* worms raised on bacteria carrying L4440 (top) or *daf-16(RNAi)*-inducing (bottom) plasmids. For L4440 and *daf-16* RNAi, respectively, seven out of seven and nine out of nine successfully ablated gonads were underdeveloped as adults. Unoperated gonad arms from operated animals developed normally, as did an additional 14 L4440 and 24 *daf-16* RNAi unoperated control worms. Scale bar: 20 μm.

suggesting that their activity might not be sufficient to drive the germline cell cycle (see Table S3 in the supplementary material). Alternatively, overexpression might not cause increased levels of active ligand because of post-transcriptional regulation (e.g. RNA stability, translation, or ligand processing, secretion or stability).

Surprisingly, the cumulative effect on the number of adult germ cells in the proliferative zone in each deletion mutant (*ins-3* and *ins-33*) was less severe than that caused by the corresponding RNAi treatments, whereas the defect in larval mitotic index was similar to that caused by the RNAi. Genome scanning revealed no obvious off-target candidates (*ins-3* matches 19 bp in T10G3.4, and *ins-33* matches 21 bp in C44C10.2, a likely pseudogene). Furthermore, neither *ins-3(RNAi)* in *ins-3(0)* nor *ins-33(RNAi)* in the *ins-33(0)* mutant produced a more severe phenotype than did the mutants alone, suggesting that the mutations and RNAi are targeting identical genes (Fig. 4C). Possibly, reducing the activity of these genes may cause a stronger phenotype than removing them; the germ line may compensate for the loss (but not the reduction) of *ins-3* or *ins-33* over time. Moreover, neither mutant-RNAi combination (Fig. 4C) nor the *ins-33;ins-3* double mutant (see Table S3 in the supplementary material) exacerbated the proliferation phenotype.

In summary, *ins-3* and *ins-33* act similarly, upstream of the *daf-2* pathway, and largely account for the effects of *daf-2*-mediated signaling on the larval germline cell cycle.

The sheath role in promoting robust larval germ cell proliferation is *daf-16* independent

Previous results indicated that the somatic gonadal sheath (especially the distal-most pair of sheath cells) is required for robust larval germline proliferation (Killian and Hubbard, 2005; McCarter et al., 1997). We considered the possibility that *ins-3* or *ins-33* could be the sheath signal. Using reporters, we did not detect *ins-3* or *ins-33* in the sheath/spermatheca lineage of the somatic gonad. Rather, *ins-3* expression was largely neuronal, whereas *ins-33* expression was largely hypodermal (see Fig. S6 in the supplementary material). However, it remains possible that expression in other tissues is below the level of detection.

To test directly whether IIR promotion of germline proliferation requires the gonadal sheath, regardless of the anatomical source of the *ins-3* and *ins-33* ligands, we ablated the sheath in the presence and absence of *daf-16* activity. Because reduction of *daf-16* restores germ cell proliferation even when *daf-2* is reduced, we reasoned that, if the sheath cells mediate IIR signaling, then unless the sheath produces another essential factor for germline proliferation, the effects of ablating the sheath should be similarly abrogated when *daf-16* is reduced. We ablated both SS cells (sheath/spermatheca precursors) and found that the ablations had similar effects in both *daf-16(+)* and *daf-16(RNAi)* animals (Fig. 5). Thus, unlike the defect in germline proliferation caused by reduced IIR signaling, the effects of ablating the sheath are not dependent on *daf-16*, which suggests that IIR signaling is not the sole essential sheath proliferation-promoting mechanism.

The effect of IIR signaling on the germ line is separable from its effects on other processes

The anatomical focus of activity for IIR signaling for dauer control is largely neuronal (Apfeld and Kenyon, 1998; Wolkow et al., 2000), whereas the anatomical focus for lifespan is predominantly intestinal (Libina et al., 2003). Therefore, the different phenotypical effects of IIR pathway mutants might correlate with tissue-specificity of the IIR response. Another, not mutually exclusive, hypothesis is that different ligands elicit different responses – either by virtue of their source, sequence of action, or interactions with other ligands or co-receptors (Murphy, 2006). We tested both of these ideas. Because previous results connect IIR signaling components with germline proliferation control in dauer (Narbonne and Roy, 2006) and with reproductive timing (Dillin et al., 2002), and because additional studies link germline proliferation with lifespan, we particularly wished to establish whether the effect of *ins-3*, *ins-33* and IIR signaling on larval germline proliferation is related to *daf-2* activities associated with the dauer decision, reproductive timing, and lifespan regulation.

First, we tested whether reducing *ins-3* or *ins-33* could cause dauer under conditions that elicit dauer by *daf-2(RNAi)*. We found that neither mutation nor RNAi treatment elevated the percentage of animals entering dauer at 27°C (see Table S4C in the supplementary material), suggesting that *ins-3* and *ins-33* do not act individually as *daf-2* agonists for the dauer decision.

Next, we investigated whether loss of *ins-3* or *ins-33* prolongs the reproductive period. We speculated that the reproductive timing phenotype of *daf-2* could be a consequence of reduced larval germline proliferation, consistent with a sensitive period for this reproductive phenotype during larval stages (Dillin et al., 2002). We measured progeny production in *daf-2*, *ins-3* and *ins-33* mutants in the presence or absence of *daf-16*. We found that unlike *daf-2*, neither *ins-3* nor *ins-33* mutants displayed delayed or prolonged reproduction (Fig. 6A). Therefore, extension of the reproductive period in *daf-2* mutants is not likely to be a secondary consequence of reduced germline proliferation in larval stages, and these phenotypes are separable.

If *ins-3* and *ins-33* act globally to activate *daf-2*, their removal should cause similar changes in *daf-16* activity in the intestine as does removal of *daf-2*. Similar to previous results (Libina et al., 2003; Lin et al., 2001), we found that reducing *daf-2* activity by RNAi caused nuclear enrichment of DAF-16::GFP and induction of *sod-3::GFP* expression. By contrast, neither effect was observed when worms were treated with *ins-3* or *ins-33* RNAi (Fig. 6B). These results suggest that *ins-3* and *ins-33* do not act individually on the *daf-2* pathway in the intestine.

Taken together with the results of temperature-shift experiments (Fig. 1A), these results are consistent with the hypothesis that the requirement for the IIR pathway regulating larval germline

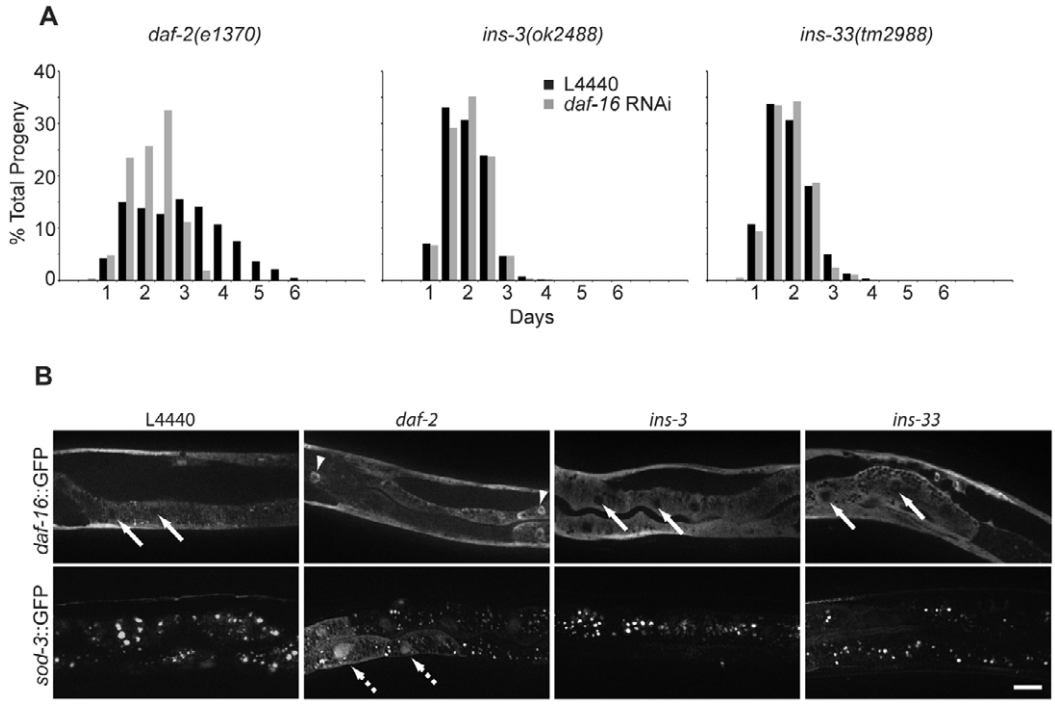

Fig. 6. *ins-3* and *ins-33* mutations do not extend the reproductive period and are not required for *daf-2*-mediated effects on DAF-16 in the intestine. (**A**) Progeny counts in *daf-2(e1370)*, *ins-3(ok2488)* and *ins-33(tm2988)*. The percentage of total progeny at each time point is shown. Black, L4440; gray, *daf-16* RNAi. Average brood sizes (*n*) for L4440 and *daf-16* RNAi, respectively: *daf-2(e1370)*, 303±12.1 (10) and 317±7.9 (10); *ins-3(ok2488)*, 265±35 (9) and 256±44 (10); *ins-33(tm2988)*, 295±13 (9) and 250±25 (9). (**B**) Intestines of representative worms expressing either DAF-16::GFP (top) or *sod-3::GFP* (bottom) grown on the indicated RNAi-inducing bacteria. Top row: arrows indicate nuclei devoid of DAF-16::GFP; arrowheads indicate nuclearly localized DAF-16::GFP. Bottom row: dotted-line arrows indicate *sod-3::GFP* expression. Scale bar: 20 μm.

proliferation is temporally and anatomically distinct from its role in dauer and other phenotypes, and that different ligands preferentially regulate different *daf-2*-dependent processes.

DISCUSSION

We uncovered a role for the canonical DAF-2/IIR pathway in promoting robust larval germline proliferation, and found that this role is distinct from that of GLP-1/Notch. These results contrast with a previous study on the neuronal role of Notch in dauer recovery that suggested that IIR signaling may be epistatic to LIN-12/Notch activity (Ouellet et al., 2008).

We identified and characterized two putative DAF-2 agonists, *ins-3* and *ins-33*, that are required in the soma to promote robust larval germline proliferation in a *daf-18*- and *daf-16*-dependent manner. Our data are consistent with a model in which activation of *daf-2* signaling in response to specific ligands (*ins-3*, *ins-33*) at a distinct period (the L3 and L4) and in a distinct tissue (the germ line) underlies the effect of this pathway on larval germline proliferation. These findings suggest the existence of special regulatory controls at this crucial time of germline proliferation. In support of this model, we found that *ins-3* and *ins-33* do not individually affect the dauer decision, reproductive timing, or intestinal DAF-16 nuclear localization or *sod-3* expression, that the effect of IIR signaling on the germline is after the dauer decision and before adulthood, and that its tissue requirement is distinct from its other roles (mainly germ line and neither neuronal nor intestinal).

ins-33 has been identified previously in two other contexts: as a direct target of the *lin-14* transcriptional repressor in the L1 (Hristova et al., 2005); and as a target of TGFβ signaling by microarray analysis. Mutations in *lin-14* cause precocious dauer programs, suggesting a possible role for *ins-33* in dauer timing or development. However, neither the results of Hristova et al. nor those of this study indicate a dauer role for *ins-33* alone. Liu et al. found that *ins-33* was upregulated together with *ins-18*, a gene proposed to act as an antagonist of *daf-2* signaling (Liu et al., 2004). Our studies, however, implicate *ins-33* as an agonist. It is possible that *ins-33* has different roles in different developmental times and contexts.

Reducing the activity of either *ins-3* or *ins-33* causes very similar germline proliferation phenotypes, and reducing both does not further exacerbate the phenotype. One interpretation of these results is that the two function together. Alternatively, they could act in series, triggering successive signaling pathways. However, exclusive DAF-2 pathway feedback is not easily reconciled with a predominantly germline-autonomous role. Alternatively, these two ligands could bind non-DAF-2 receptors and act in a signal relay. The family of insulin-related ligands in humans, some of which do not bind the insulin receptor or IGFRs [e.g. relaxins (Bathgate et al., 2005)], are structurally related to only one class of the putative *C. elegans* insulin-like peptides (Pierce et al., 2001). Also, a bioinformatics study suggested the existence of *C. elegans* genes with possible similarity to the extracellular domain of IIRs (Dlakic, 2002). Although there may be considerable redundancy among the 40 insulin-like peptides in the *C. elegans* genome, it will be interesting to resolve their roles in relation to *daf-2* activity. Regardless of the precise mechanism, taken together with previous studies (Apfeld and Kenyon, 1998; Libina et al., 2003; Murphy et al., 2007; Wolkow et al., 2000), our data support a model in which different phenotypes are associated with specific ligands and target tissues.

Previous studies implicate *daf-2* pathway components in other aspects of germline proliferation. Narbonne and Roy showed that DAF-2/IIR and DAF-7/TGFβ converge on DAF-18/PTEN to prevent inappropriate germline proliferation under dauer-inducing conditions (Narbonne and Roy, 2006). Fukuyama et al. demonstrated *daf-18*-dependent germline cell cycle arrest in the starvation-induced L1 diapause (Fukuyama et al., 2006). In both cases, cell cycle arrest is *daf-16* independent and occurs in G2 (Fukuyama et al., 2006; Narbonne and Roy, 2006). We found that under non-starvation conditions, the effect of reducing IIR signaling on larval germline proliferation is dependent on both *daf-18* and *daf-16*, and that it also affects the G2.

Our studies suggest that the DAF-2 pathway acts independently of both GLP-1/Notch and the sheath to promote robust larval germline proliferation. Because GLP-1 signaling is required to maintain germ cells in an undifferentiated (mitotic) state as opposed to a differentiated (meiotic) state (Austin and Kimble, 1987), it is difficult to separate its contribution to cell cycle from its role in the mitosis/meiosis decision. Our results suggest that the role of GLP-1 in promoting larval germline proliferation is primarily to prevent differentiation. Although we found that reducing *glp-1* activity did not reduce the mitotic index of remaining cycling larval germ cells, elevating GLP-1 signaling elevates the mitotic index of germ cells that are cycling in adults (Berry et al., 1997; Maciejowski et al., 2006). Therefore it is likely, as suggested by Berry et al. (Berry et al., 1997), that positive feedback exists between mitotically active cells and *glp-1*. Moreover, additional cell cycle controls are likely to act in conjunction with GLP-1 in the adult.

Recent studies suggest a role for IIR signaling in tumor growth. In *C. elegans*, Pinkston et al. observed that reducing *daf-2* activity lowered the mitotic index in germline tumors in adult *gld-1*-mutants (Pinkston et al., 2006). Strikingly, mitotic index was reduced within the tumor, but not in the distal proliferative zone. Our data are consistent with these results, as we do not observe a defect in adult germline proliferation in *daf-2* mutants. Taken together with the Pinkston et al. study (Pinkston et al., 2006), our results suggest that germline tumor growth control in *gld-1* mutants may more closely resemble that of the larval germ line.

Our data further suggest that a role for IIR in nutrition-sensitive cell proliferation control might be widely conserved. In mammals, IIR signaling through PTEN can influence tumor growth sensitivity to short-term dietary restriction (Kalaany and Sabatini, 2009). In *Drosophila*, insulin-FOXO signaling controls germline stem cell proliferation in response to rich dietary conditions. Similar to our findings, receptor signaling is required in the germ line and impinges on G2 (Drummond-Barbosa and Spradling, 2001; LaFever and Drummond-Barbosa, 2005; Hsu et al., 2008). These parallels suggest that IIR signaling may be a conserved mechanism to tie nutrition to cell cycle control. We speculate that *C. elegans* larvae, having embarked on a reproductive (as opposed to dauer) developmental path, make an assessment of nutritional sufficiency, and that this information influences germline proliferation. It will be of interest to further test this hypothesis, as it would provide a simple model system in which to study the link between nutrition, metabolism and cell proliferation.

Acknowledgements
We thank Tim Schedl, Paul Fox, Ann Wehman, Jeremy Nance, the *C. elegans* Gene Knockout Consortium (Oklahoma City and Vancouver, Canada), the *Caenorhabditis* Genetics Center (CGC, Minneapolis, MN; funded by NIH NCRR), and the National Bioresource Project for the Nematode *C. elegans* (Tokyo, Japan) for strains and/or advice; Cathy Wolkow, Monica Driscoll, Michael Glotzer, and Thomas Johnson for plasmids; Shai Shaham for help with expression pattern analysis; Bernard Lakowski and Dan Tranchina for help with statistics; and John Maciejowski for excellent technical assistance. We especially thank Roumen Voutev for input on many aspects of the work and all members of Hubbard and Nance labs for helpful discussions. Funding was provided by NIH grant R01GM61706 to E.J.A.H. Deposited in PMC for release after 12 months.

Competing interests statement
The authors declare no competing financial interests.

Supplementary material
Supplementary material for this article is available at
http://dev.biologists.org/lookup/suppl/doi:10.1242/dev.042523/-/DC1

References

Apfeld, J. and Kenyon, C. (1998). Cell nonautonomy of C. elegans daf-2 function in the regulation of diapause and life span. *Cell* **95**, 199-210.
Austin, J. and Kimble, J. (1987). glp-1 is required in the germ line for regulation of the decision between mitosis and meiosis in C. elegans. *Cell* **51**, 589-599.
Bathgate, R. A., Ivell, R., Sanborn, B. M., Sherwood, O. D. and Summers, R. J. (2005). Receptors for relaxin family peptides. *Ann. N Y Acad. Sci.* **1041**, 61-76.
Baumeister, R., Schaffitzel, E. and Hertweck, M. (2006). Endocrine signaling in Caenorhabditis elegans controls stress response and longevity. *J. Endocrinol.* **190**, 191-202.
Berry, L. W., Westlund, B. and Schedl, T. (1997). Germ-line tumor formation caused by activation of glp-1, a Caenorhabditis elegans member of the Notch family of receptors. *Development* **124**, 925-936.
Brenner, S. (1974). The genetics of Caenorhabditis elegans. *Genetics* **77**, 71-94.
Crittenden, S. L., Leonhard, K. A., Byrd, D. T. and Kimble, J. (2006). Cellular analyses of the mitotic region in the Caenorhabditis elegans adult germ line. *Mol. Biol. Cell* **17**, 3051-3061.
Dillin, A., Crawford, D. K. and Kenyon, C. (2002). Timing requirements for insulin/IGF-1 signaling in C. elegans. *Science* **298**, 830-834.
Dlakic, M. (2002). A new family of putative insulin receptor-like proteins in C. elegans. *Curr. Biol.* **12**, R155-R157.
Dorsett, M., Westlund, B. and Schedl, T. (2009). METT-10, A Putative Methyltransferase, Inhibits Germ Cell Proliferative Fate in Caenorhabditis elegans. *Genetics* **183**, 233-247.
Drummond-Barbosa, D. and Spradling, A. C. (2001). Stem cells and their progeny respond to nutritional changes during Drosophila oogenesis. *Dev. Biol.* **231**, 265-278.
Eckmann, C. R., Crittenden, S. L., Suh, N. and Kimble, J. (2004). GLD-3 and control of the mitosis/meiosis decision in the germline of Caenorhabditis elegans. *Genetics* **168**, 147-160.
Edgar, B. A. (2006). How flies get their size: genetics meets physiology. *Nat. Rev. Genet.* **7**, 907-916.
Edgar, B. A. and Lehner, C. F. (1996). Developmental control of cell cycle regulators: a fly's perspective. *Science* **274**, 1646-1652.
Feng, H., Zhong, W., Punkosdy, G., Gu, S., Zhou, L., Seabolt, E. K. and Kipreos, E. T. (1999). CUL-2 is required for the G1-to-S-phase transition and mitotic chromosome condensation in Caenorhabditis elegans. *Nature Cell Biol.* **1**, 486-492.
Fichelson, P., Audibert, A., Simon, F. and Gho, M. (2005). Cell cycle and cell-fate determination in Drosophila neural cell lineages. *Trends Genet.* **21**, 413-420.
Fielenbach, N. and Antebi, A. (2008). C. elegans dauer formation and the molecular basis of plasticity. *Genes Dev.* **22**, 2149-2165.
Fukuyama, M., Rougvie, A. E. and Rothman, J. H. (2006). C. elegans DAF-18/PTEN mediates nutrient-dependent arrest of cell cycle and growth in the germline. *Curr. Biol.* **16**, 773-779.
Gami, M. S. and Wolkow, C. A. (2006). Studies of Caenorhabditis elegans DAF-2/insulin signaling reveal targets for pharmacological manipulation of lifespan. *Aging Cell* **5**, 31-37.
Gems, D., Sutton, A. J., Sundermeyer, M. L., Albert, P. S., King, K. V., Edgley, M. L., Larsen, P. L. and Riddle, D. L. (1998). Two pleiotropic classes of daf-2 mutation affect larval arrest, adult behavior, reproduction and longevity in Caenorhabditis elegans. *Genetics* **150**, 129-155.
Gil, E. B., Malone Link, E., Liu, L. X., Johnson, C. D. and Lees, J. A. (1999). Regulation of the insulin-like developmental pathway of Caenorhabditis elegans by a homolog of the PTEN tumor suppressor gene. *Proc. Natl. Acad. Sci. USA* **96**, 2925-2930.
Gottlieb, S. and Ruvkun, G. (1994). daf-2, daf-16 and daf-23: genetically interacting genes controlling Dauer formation in Caenorhabditis elegans. *Genetics* **137**, 107-120.
Gumienny, T. L., Lambie, E., Hartwieg, E., Horvitz, H. R. and Hengartner, M. O. (1999). Genetic control of programmed cell death in the Caenorhabditis elegans hermaphrodite germline. *Development* **126**, 1011-1022.

Hanahan, D. and Weinberg, R. A. (2000). The hallmarks of cancer. *Cell* **100**, 57-70.
Hansen, D., Wilson-Berry, L., Dang, T. and Schedl, T. (2004). Control of the proliferation versus meiotic development decision in the C. elegans germline through regulation of GLD-1 protein accumulation. *Development* **131**, 93-104.
Henderson, S. T. and Johnson, T. E. (2001). daf-16 integrates developmental and environmental inputs to mediate aging in the nematode Caenorhabditis elegans. *Curr. Biol.* **11**, 1975-1980.
Henderson, S. T., Gao, D., Lambie, E. J. and Kimble, J. (1994). lag-2 may encode a signaling ligand for the GLP-1 and LIN-12 receptors of C. elegans. *Development* **120**, 2913-2924.
Hill, A. A., Hunter, C. P., Tsung, B. T., Tucker-Kellogg, G. and Brown, E. L. (2000). Genomic analysis of gene expression in C. elegans. *Science* **290**, 809-812.
Hirsh, D., Oppenheim, D. and Klass, M. (1976). Development of the reproductive system of Caenorhabditis elegans. *Dev. Biol.* **49**, 200-219.
Hristova, M., Birse, D., Hong, Y. and Ambros, V. (2005). The Caenorhabditis elegans heterochronic regulator LIN-14 is a novel transcription factor that controls the developmental timing of transcription from the insulin/insulin-like growth factor gene ins-33 by direct DNA binding. *Mol. Cell Biol.* **25**, 11059-11072.
Hsu, H. J., LaFever, L. and Drummond-Barbosa, D. (2008). Diet controls normal and tumorous germline stem cells via insulin-dependent and –independent mechanisms in Drosophila. *Dev. Biol.* **313**, 700-712.
Hu, P. (2007). Dauer (August 08, 2007), WormBook, ed. The C. elegans Research Community, WormBook, doi/10.1895/wormbook.1.144.1, http://www.wormbook.org.
Kalaany, N. Y. and Sabatini, D. M. (2009). Tumours with PI3K activation are resistant to dietary restriction. *Nature* **458**, 725-731.
Kelly, W. G., Xu, S., Montgomery, M. K. and Fire, A. (1997). Distinct requirements for somatic and germline expression of a generally expressed Caernorhabditis elegans gene. *Genetics* **146**, 227-238.
Kenyon, C., Chang, J., Gensch, E., Rudner, A. and Tabtiang, R. (1993). A C. elegans mutant that lives twice as long as wild type. *Nature* **366**, 461-464.
Killian, D. J. and Hubbard, E. J. (2004). C. elegans pro-1 activity is required for soma/germline interactions that influence proliferation and differentiation in the germ line. *Development* **131**, 1267-1278.
Killian, D. J. and Hubbard, E. J. (2005). Caenorhabditis elegans germline patterning requires coordinated development of the somatic gonadal sheath and the germ line. *Dev. Biol.* **279**, 322-335.
Kimura, K. D., Tissenbaum, H. A., Liu, Y. and Ruvkun, G. (1997). daf-2, an insulin receptor-like gene that regulates longevity and diapause in Caenorhabditis elegans. *Science* **277**, 942-946.
Kohlmaier, A. and Edgar, B. A. (2008). Proliferative control in Drosophila stem cells. *Curr. Opin. Cell Biol.* **20**, 699-706.
LaFever, L. and Drummond-Barbosa, D. (2005). Direct control of germline stem cell division and cyst growth by neural insulin in Drosophila. *Science* **309**, 1071-1073.
Larsen, P. L., Albert, P. S. and Riddle, D. L. (1995). Genes that regulate both development and longevity in Caenorhabditis elegans. *Genetics* **139**, 1567-1583.
Li, C. and Kim, K. (2008). Neuropeptides (September 25, 2008), WormBook, ed. The C. elegans Research Community, WormBook, doi/10.1895/wormbook.1.142.1, http://www.wormbook.org.
Li, J., Ebata, A., Dong, Y., Rizki, G., Iwata, T. and Lee, S. S. (2008). Caenorhabditis elegans HCF-1 functions in longevity maintenance as a DAF-16 regulator. *PLoS Biol.* **6**, e233.
Li, W., Kennedy, S. G. and Ruvkun, G. (2003). daf-28 encodes a C. elegans insulin superfamily member that is regulated by environmental cues and acts in the DAF-2 signaling pathway. *Genes Dev.* **17**, 844-858.
Libina, N., Berman, J. R. and Kenyon, C. (2003). Tissue-specific activities of C. elegans DAF-16 in the regulation of lifespan. *Cell* **115**, 489-502.
Lin, K., Dorman, J. B., Rodan, A. and Kenyon, C. (1997). daf-16: An HNF-3/forkhead family member that can function to double the life-span of Caenorhabditis elegans. *Science* **278**, 1319-1322.
Lin, K., Hsin, H., Libina, N. and Kenyon, C. (2001). Regulation of the Caenorhabditis elegans longevity protein DAF-16 by insulin/IGF-1 and germline signaling. *Nat. Genet.* **28**, 139-145.
Liu, T., Zimmerman, K. K. and Patterson, G. I. (2004). Regulation of signaling genes by TGFbeta during entry into dauer diapause in C. elegans. *BMC Dev. Biol.* **4**, 11.
Maciejowski, J., Ugel, N., Mishra, B., Isopi, M. and Hubbard, E. J. (2006). Quantitative analysis of germline mitosis in adult C. elegans. *Dev. Biol.* **292**, 142-151.
Malone, E. A. and Thomas, J. H. (1994). A screen for nonconditional dauer-constitutive mutations in Caenorhabditis elegans. *Genetics* **136**, 879-886.
McCarter, J., Bartlett, B., Dang, T. and Schedl, T. (1997). Soma-germ cell interactions in Caenorhabditis elegans: multiple events of hermaphrodite germline development require the somatic sheath and spermathecal lineages. *Dev. Biol.* **181**, 121-143.
McGovern, M., Voutev, R., Maciejowski, J., Corsi, A. K. and Hubbard, E. J. A. (2009). A "latent niche" mechanism for tumor initiation. *Proc. Natl. Acad. Sci. USA* **106**, 11617-11622.
Murphy, C. T. (2006). The search for DAF-16/FOXO transcriptional targets: approaches and discoveries. *Exp. Gerontol.* **41**, 910-921.
Murphy, C. T., Lee, S. J. and Kenyon, C. (2007). Tissue entrainment by feedback regulation of insulin gene expression in the endoderm of Caenorhabditis elegans. *Proc. Natl. Acad. Sci. USA* **104**, 19046-19050.
Nadarajan, S., Govindan, J. A., McGovern, M., Hubbard, E. J. and Greenstein, D. (2009). MSP and GLP-1/Notch signaling coordinately regulate actomyosin-dependent cytoplasmic streaming and oocyte growth in C. elegans. *Development* **136**, 2223-2234.
Narbonne, P. and Roy, R. (2006). Inhibition of germline proliferation during C. elegans dauer development requires PTEN, LKB1 and AMPK signalling. *Development* **133**, 611-619.
Ogg, S. and Ruvkun, G. (1998). The C. elegans PTEN homolog, DAF-18, acts in the insulin receptor-like metabolic signaling pathway. *Mol. Cell* **2**, 887-893.
Ogg, S., Paradis, S., Gottlieb, S., Patterson, G. I., Lee, L., Tissenbaum, H. A. and Ruvkun, G. (1997). The Fork head transcription factor DAF-16 transduces insulin-like metabolic and longevity signals in C. elegans. *Nature* **389**, 994-999.
Orford, K. W. and Scadden, D. T. (2008). Deconstructing stem cell self-renewal: genetic insights into cell-cycle regulation. *Nat. Rev. Genet.* **9**, 115-128.
Ouellet, J., Li, S. and Roy, R. (2008). Notch signalling is required for both dauer maintenance and recovery in C. elegans. *Development* **135**, 2583-2592.
Patel, D. S., Garza-Garcia, A., Nanji, M., McElwee, J. J., Ackerman, D., Driscoll, P. C. and Gems, D. (2008). Clustering of genetically defined allele classes in the Caenorhabditis elegans DAF-2 insulin/IGF-1 receptor. *Genetics* **178**, 931-946.
Pepper, A. S., Killian, D. J. and Hubbard, E. J. (2003). Genetic analysis of Caenorhabditis elegans glp-1 mutants suggests receptor interaction or competition. *Genetics* **163**, 115-132.
Pierce, S. B., Costa, M., Wisotzkey, R., Devadhar, S., Homburger, S. A., Buchman, A. R., Ferguson, K. C., Heller, J., Platt, D. M., Pasquinelli, A. A. et al. (2001). Regulation of DAF-2 receptor signaling by human insulin and ins-1, a member of the unusually large and diverse C. elegans insulin gene family. *Genes Dev.* **15**, 672-686.
Pinkston, J. M., Garigan, D., Hansen, M. and Kenyon, C. (2006). Mutations that increase the life span of C. elegans inhibit tumor growth. *Science* **313**, 971-975.
Rouault, J. P., Kuwabara, P. E., Sinilnikova, O. M., Duret, L., Thierry-Mieg, D. and Billaud, M. (1999). Regulation of dauer larva development in Caenorhabditis elegans by daf-18, a homologue of the tumour suppressor PTEN. *Curr. Biol.* **9**, 329-332.
Sancho, E., Batlle, E. and Clevers, H. (2004). Signaling pathways in intestinal development and cancer. *Annu. Rev. Cell Dev. Biol.* **20**, 695-723.
Seydoux, G., Savage, C. and Greenwald, I. (1993). Isolation and characterization of mutations causing abnormal eversion of the vulva in Caenorhabditis elegans. *Developmental Biology* **157**, 423-436.
Sijen, T., Fleenor, J., Simmer, F., Thijssen, K. L., Parrish, S., Timmons, L., Plasterk, R. H. and Fire, A. (2001). On the role of RNA amplification in dsRNA-triggered gene silencing. *Cell* **107**, 465-476.
Taguchi, A. and White, M. F. (2008). Insulin-like signaling, nutrient homeostasis, and life span. *Annu. Rev. Physiol.* **70**, 191-212.
Timmons, L., Court, D. L. and Fire, A. (2001). Ingestion of bacterially expressed dsRNAs can produce specific and potent genetic interference in Caenorhabditis elegans. *Gene* **263**, 103-112.
Tissenbaum, H. A. and Ruvkun, G. (1998). An insulin-like signaling pathway affects both longevity and reproduction in Caenorhabditis elegans. *Genetics* **148**, 703-717.
Vowels, J. J. and Thomas, J. H. (1992). Genetic analysis of chemosensory control of dauer formation in Caenorhabditis elegans. *Genetics* **130**, 105-123.
Wolkow, C. A., Kimura, K. D., Lee, M. S. and Ruvkun, G. (2000). Regulation of C. elegans life-span by insulinlike signaling in the nervous system. *Science* **290**, 147-150.

Table S1. Strains

A Strains used for experiments presented in main text

Strain	Genotype	Reference/Source
CB1370	*daf-2(e1370)*	(Riddle et al., 1981)
DR1567	*daf-2(m577)*	(Gems et al., 1998)
DR1572	*daf-2(e1368)*	(Gems et al., 1998)
CF1553	*muIs84 [pAD76 (sod-3::GFP)]*	(Libina et al., 2003)
CF1038	*daf-16(mu86)*	(Lin et al., 1997)
CB4037	*glp-1 (e2141)*	(Priess et al., 1987)
PD8488	*rrf-1(pk1417)*	(Sijen et al., 2001)
GC678	*tnIs6[lim-7::GFP; rol-6 (su1006)]; qIs19[lag-2::GFP; rol-6(su1006)*]	(Killian and Hubbard, 2004)
GC888	*glp-1(bn18)*	(Kodoyianni et al., 1992)
GC833	*glp-1(ar202)*	(Pepper et al., 2003a)
RB712	*daf-18(ok480)*	*C. elegans* Gene Knockout Consortium, Oklahoma City and Vancouver, Canada, and the *Caenorhabditis* Genetics Center (CGC), Minneapolis, MN, USA
CF1295	*daf-16(mu86) I; daf-2(e1370) III; muEx108[pKL99-2(DAF-16::GFP/daf16bKO) + pRF4(rol-6(su1006)]*	(Lin et al., 2001)
GC1019	*rrf-1(pk1417);daf-2(e1370)*	This work
GC854	*daf-2(e1370); glp-1(e2141)*	This work
GC1071	*ins-3(ok2488)* [a]	This work: 2x backcross of RB1915; *C. elegans* Gene Knockout Consortium and the CGC [a]
GC1039	*ins-33(tm2988)*	This work: 8x backcross of FX02988; National Bioresource Project for the Nematode *C. elegans,* Tokyo, Japan
GC865	*daf-16(mu86); muEx108[pKL99-2(daf-16::GFP/daf16bKO) + pRF4(rol-6(su1006))]*	This work: constructed from CF1038 *daf-16(mu86)* (Lin et al., 1997) and CF1295 *daf-16(mu86) I; daf-2(e1370) III; muEx108[pKL99-2(DAF-6::GFP/daf16bKO) + pRF4(rol-6(su1006)]* (Lin et al., 2001), this fusion uses isoform a of *daf-16* and contains a stop codon before isoform b
GC1079	*ins-3(ok2488); naEx187*[pGC467, pRF4] [b]	This work
GC1078	*ins-33(tm2988); naEx186*[pGC464; pRF4] [b]	This work
GC1087	*ins-33(tm2988); naEx195*[pGC464; pRF4] [b]	This work
GC1089	*ins-33(tm2988); naEx197*[pGC464; pRF4] [b]	This work
DR1309	*daf-16(m26); daf-2(e1370)*	P. Albert and D. Riddle, via CGC
CF1442	*daf-16(mu86);daf-2(e1370); muEx169[Punc-119::GFP::DAF-16* + pRF4 *rol-6 (su1006)]*	(Libina et al., 2003)
CF1514	*daf-16(mu86); daf-2(e1370); muEx211[*pNL213 *(Pges-1::GFP::DAF-16)* + pRF4 *rol-6 (su1006)]*	(Libina et al., 2003)
CF1515	*daf-16(mu86); daf-2(e1370); muEx212[*pNL212 *(Pmyo-3::GFP::DAF-16)* + pRF4 *rol-6 (su1006)]*	(Libina et al., 2003)
GC1143	*unc-119(ed3)III; naIs43[pGC492(Prpl-11.1::daf-16cDNA::GFP::nos-2 3'UTR – unc-119(+))]* [c]	This work: microparticle bombardment (Praitis et al., 2001) of DP38 worms with pGC492
GC1144	*daf-16(mu86)I;daf-2(e1370)III; naIs43[pGC492(Prpl-11.1::daf-16cDNA::GFP::nos2 3'UTR unc-119(+))]* [c]	This work: generated by crossing GC1143 with DR1309
GC1109	*daf-16(m26) I ; daf-2(e1370) II ; naEx202 [pGC461 (Plag-2::daf-16::GFP) + pRF4]*	This work: *pGC461 was injected to DR1309*
RB777	*hcf-1(ok559)*	*C. elegans* Gene Knockout Consortium, and the CGC
GC1109	*naEx202*[pGC461; pRF4] [d]	This work
GC1004	*ins-33(tm2988)* cross	This work: taken from spontaneous male from GC1039
GC585	*pro-1(na48)/mIn1[dpy-10(e128) mIs14]*	Used as a carrier of the *mIs14* balancer
GC1142	*ins-33(tm2988);ins-3(ok2488)*	This work: generated by crossing GC1004 males to GC1071; using GC585 to balance *ins-3*

B Strains used for data presented in supplementary material

Strain	Genotype	Reference/Source
CB1375	*daf-18(e1375)*	(Riddle et al., 1981)
FT224	*xnIs87* [pMP322 *(Psyn-4::GFP-syn-4::syn-4 3' UTR); unc-119 (+)]; syn-4 tag-316(ok372) IV*	Gift from Ann Wehman and Jeremy Nance; pMP322 gift from Michael Glotzer; *ok372* removes both *syn-4* and *tag-316*
GC967	*daf-16(mu86); glp-1(ar202); naEx148* [pGP30(DAF-16::GFP) + *sur-5::GFP*]	This work: injection of GC908 *daf-16(mu86); glp-1(ar202)* with pGP30 (Henderson and Johnson, 2001) at 1ng/μl; *sur-5::GFP* at 20ng/μl; and pBluescript DNA at 80ng/μl; DAF-16 sequences in pGP30 correspond to isoform a2
GC1112	*daf-16(mu86); daf-2(e1370); naEx148* [pGP30(DAF-16::GFP) + *sur-5::GFP*]	This work: generated by crossing GC967 with DR1309 males and selecting for GFP-positive dauer worms and selecting against *glp-1(ar202)*
GC1080	*smg-1(cc546); naEx188*[pGC487; pRF4] [e]	This work
GC1081	*smg-1(cc546); naEx189*[pGC487; pRF4] [e]	This work
GC1082	*smg-1(cc546); naEx190*[pGC486; pRF4] [e]	This work
GC1083	*smg-1(cc546); naEx191*[pGC486; pRF4] [e]	This work
GC1084	*smg-1(cc546); naEx192*[pGC486; pRF4] [e]	This work
GC1085	*smg-1(cc546); naEx193*[pGC486; pRF4] [e]	This work
GC1088	*naEx196*[pGC467; pRF4] [f]	This work
GC1095	*naEx198*[pGC467; pRF4] [f]	This work
GC1076	*naEx184*[pGC464; pRF4] [f]	This work
GC1077	*naEx185*[pGC464; pRF4] [f]	This work
GC1145	*daf-2(e1370);xnIs879pMP322(Psyn-4::GFP::syn-4::syn-4 3'UTR)unc-119(+)];syn-4 tag-316(ok372)*	This work: generated by crossing FT224 with CB1370

[a] Three out of 12 *ins-3(ok2488)* worms examined for the brood size analysis shown in Fig. 6 laid exclusively dead embryos, presumably due to a maternal effect lethal mutation in the background. They were not included in the analysis.

[b] Rescuing (pGC) plasmids were injected at 10 ng/μl together with 100 ng/μl of the transformation marker pRF4 [*(rol-6(su1006)*].

[c] The presence of the transgene was determined using PCR with primers to GFP. The data shown in Fig. 3C is from the line as scored shortly after it was established and expression validated by RT-PCR. However, subsequent RT-PCR indicated that expression from the transgene was becoming silenced (likely reflected in large variation of the data, see Fig. S2), and later thaws of our frozen stocks showed no expression indicating complete silencing subsequent to the experiments presented in this data collection. Measurements conducted on thawed strains (after silencing) also lost *daf-16(+)* activity.

[d] Microinjection of DR1309 was performed with 5 ng/μl of pGC461 [P*lag-2*::*daf-16*::GFP] and 100 ng/μl of pRF4 [*(rol-6(su1006)*].

[e] *ins-3* and *ins-33* rescue: (GC1080-GC1085) generated by microinjection of PD8120 *smg-1(cc546)* (A. Fire and the *Caenorhabditis* Genetics Center, Minneapolis, MN, USA) with 20 ng/μl of the (pGC) expression plasmid and 100 ng/μl of pRF4 [*(rol-6(su1006)*].

[f] *ins-3* and *ins-33* overexpression: (GC1088, GC1095 and GC1076, GC1077) microinjection of N2 was performed with 100 ng/μl of the expression plasmid and 100 ng/μl of pRF4 [*(rol-6(su1006)*].

Table S2. Plasmids

A Plasmids used for data presented in main text

Plasmid	Description	Reference/Source/Construction
pGC464	*ins-33* rescue and overexpression	This work: ~8kb genomic region of *ins-33* was PCR amplified using the following primers: AAGGAGAACAACTGTATCGAGATTTGAGGG and CATCGTCTGGAACAATGAAGAAACGAATGGGCGG and TA cloned into pCR-XL-TOPO (Invitrogen)
pGC467	*ins-3* rescue and overexpression	This work: ~11.5kb genomic region of *ins-3* was PCR amplified using the following primers: ATGAAGCGGAGAGAAGAAGTGCGGAGAGAAGG and GTTATGGACATATCGTACTAAGTCTGCTGCCC and TA- cloned into pCR-XL-TOPO (Invitrogen)
sjj_C46A5.9	*hcf-1*	(Kamath et al., 2003) [a]
sjj_T07A9.6	*daf-18*	(Kamath et al., 2003) [a]
sjj_R13H8.2 [b]	*daf-16*	(Kamath et al., 2003) [a]
sjj_R13H8.1 [b]	*daf-16*	(Kamath et al., 2003) [a]
mv_CAA10315	*daf-18*	(Rual et al., 2004; C.elegans ORF-RNAi library (Geneservice Ltd.))[a]
	RNAi-targeting: *ins-1, ins-2, ins-3*	Kindly provided by Monica Driscoll [a]
pGC488	*daf-2*	This work: created by ligating the *Kpn*I/*Xba*I fragment from pKDK33 (Wolkow et al., 2000) to similarly-digested L4440
pGC461	Distal tip cell expression of DAF-16	This work: *daf-16*::GFP fusion (gift of T. Johnson) was fused to the *lag-2* promoter in pJK590 (Blelloch et al., 1999; Mathies et al., 2003).
pGC492	Germline expression of DAF-16	This work: *daf-16*::GFP fusion (gift of T. Johnson) was fused to nos-2 3'UTR. The *rpl-11.1* promoter (5'-cgcgttcaatccccggttcggccctttttt…..tcacagttttcaaattttatgtatttatgc-3') and then cloned along with the *C. briggsae unc-119(+)* gene into pPD117.01 (kind gift of Barth Grant).

B Plasmids used for data presented in supplementary material

Plasmid	Description	Reference/Source/Construction
pGC487	*ins-3* expression	This work: A 5565 bp 5' fragment of *ins-3* was PCR amplified from pGC467 using primers: CAAGCTAGCTAAGTAAGTTGTATTTGTTACAAACG and CAAGGGCCCGTGTGAAGTCGACTTTGCAGATCAG, digested with *Nhe*I and *Apa*I, and ligated to similarly digested pGC305 (Voutev and Hubbard, 2008), to create pGC485. Next, a 5749 bp fragment covering the first intron to the 3' downstream region, was PCR amplified from pGC467 using primers: AACCTGCAGGGGTTGTCGACATGAAGCGGAGAG and CAACCCGGGTATTCAGAACAGGAATTGATAAATGTGTC, digested with *Sbf*I and *Xma*I, and ligated to similarly digested pGC485, to create pGC487
pGC486	*ins-33* expression	This work: A 1287 bp 5' fragment of *ins-33* was PCR amplified from pGC464 using the following primers: CAAGGATCCAAGGAGAACAACTGTATCGAG and CAAGAGCTCTTTTGTTCAAAAAATCAGCAC, digested with *Bam*HI and *Sac*I, and ligated to similarly digested pGC305 (Voutev and Hubbard, 2008), to create pGC482. Next, a 5800 bp fragment covering the first intron to the 3' downstream region, was PCR amplified from pGC464 using the following primers: CAAGCTAGCTAAGTAAGCGATGAAAATCGATAGAACAC and CAAGGGCCCCATCGTCTGGAACAATGAAGAAACG, digested with *Nhe*I and *Apa*I, and ligated to similarly digested pGC482, to create pGC486
	RNAi-targeting: *ins-4, ins-5 ins-6, ins-8, ins-9, ins-10, ins-11 ins-12, ins-13, ins-14, ins-15, ins-16, ins-17, ins-18, ins-19, ins-20, ins-21, ins-22, ins-23, ins-26, ins-27, ins-28, ins-29, ins-30, ins-32, ins-33, ins-34, ins-35, ins-36, ins-37*	Kindly provided by Monica Driscoll [a]
sjj_F21E9.4	*ins-39*	(Kamath et al., 2003) [a]
pGC314	*ins-7*	This work [c]: ATATTCTAGAATGCCACCAATAATTTTGG and ATATCTCGAGTTAAGGACAGCACTGTTTTC
pGC315	*ins-24*	This work [c]: ATATTCTAGAATGAGATCTCCCACCTTG and ATATCTCGAGTTAGAAAACGAAGCCAGATG
pGC316	*ins-31*	This work [c]: ATATTCTAGAATGAAGATGCCCTTGATC and ATATCTCGAGTCAGTAAAAGCCTGGACG
pGC317	*ins-38*	This work [c]: ATATTCTAGAATGAATCTTTTTCTCCTCG and ATATCTCGAGCTATAGCTTGCTGGGGC
pGC318	*daf-28*	This work [c]: ATATTCTAGAATGAACTGCAAGCTCATCG and ATATCTCGAGGTGGTTCACAGGCGTCTC

[a] Verified by DNA sequencing.
[b] These two reagents gave similar results.
[c] In each case, plasmids were made by PCR amplification from a cDNA library (Invitrogen) using indicated primers, digested with *Xba*I/*Xho*I, and ligated into similarly-digested L4440.

Table S3. Number of germ nuclei in the proliferative zone

Strain	Genotype	RNAi reagent	RNAi target	Number of nuclei [a]	SEM [b]	*n* [b]
N2				209.0	±3.6	33
N2		L4440		195.6	±8.4	61
N2		*ins-1* [c]	*ins-1*	187.6	±6.5	19
N2		*ins-3* [c]	*ins-3*	135.9	±6.6	39
N2		*ins-33* [c]	*ins-33*	136.9	±6.0	45
N2		sjj_C46A5.9 [d]	*hcf-1*	168.9	±3.8	24
N2		pGC488 [e]	*daf-2*	175.0	±4.4	21
N2	(male)			159.7	±6.0	19
N2	(male)	L4440		162.1	±4.4	19
N2	(male)	*ins-3* [c]	*ins-3*	130.0	±9.5	8
N2	(male)	*ins-33* [c]	*ins-33*	134.6	±9.1	9
PD8488	*rrf-1(pk1417)*	L4440		193.9	±3.7	24
PD8488	*rrf-1(pk1417)*	*ins-1* [c]	*ins-1*	187.7	±6.1	17
PD8488	*rrf-1(pk1417)*	*ins-3* [c]	*ins-3*	188.7	±4.4	12
PD8488	*rrf-1(pk1417)*	*ins-33* [c]	*ins-33*	178.8	±7.7	19
PD8488	*rrf-1(pk1417)*	sjj_C46A5.9 [d]	*hcf-1*	166.9	±3.9	21
PD8488	*rrf-1(pk1417)*	pGC488 [e]	*daf-2*	161.6	±7.4	25
CB1370	*daf-2(e1370)*			128.4	±3.6	29
CB1370	*daf-2(e1370)* (male)			110.5	±6.6	12
CB1370	*daf-2(e1370)*	L4440		140.0	±3.2	34
CB1370	*daf-2(e1370)*	*ins-3* [c]	*ins-3*	142.3	±2.3	16
CB1370	*daf-2(e1370)*	*ins-33* [c]	*ins-33*	138.3	±4.5	15
CB1370	*daf-2(e1370)*	sjj_T07A9.6 [d]	*daf-18*	176.5	±5.6	10
CB1370	*daf-2(e1370)*	mv_CAA10315 [f]	*daf-18*	184.3	±5.5	15
CB1370	*daf-2(e1370)*	sjj_R13H8.2 [d]	*daf-16*	175.5	±4.6	11
CB1370	*daf-2(e1370)*	sjj_R13H8.1 [d]	*daf-16*	182.2	±2.8	44
CB1370	*daf-2(e1370)*	sjj_C46A5.9 [d]	*hcf-1*	130.5	±5.6	14
GC1019	*rrf-1(pk1417);daf-2(e1370)*	L4440		144.9	±4.2	26
GC1019	*rrf-1(pk1417);daf-2(e1370)*	sjj_T07A9.6 [d]	*daf-18*	177.9	±4.4	11
GC1019	*rrf-1(pk1417);daf-2(e1370)*	mv_CAA10315 [f]	*daf-18*	182.6	±3.7	16
GC1019	*rrf-1(pk1417);daf-2(e1370)*	sjj_R13H8.1 [d]	*daf-16*	188.8	±4.0	36
DR1309	*daf-16(mu86); daf-2(e1370)*			194.4	±3.3	20
CF1295sib [g]	*daf-16(mu86);daf-2(e1370)*			199.1	±5.1	14
CF1295 [g]	*daf-16(mu86);daf-2(e1370); muEx108[DAF-16::GFP]*			140.5	±5.8	14
GC1112sib [g]	*daf-16(mu86); daf-2(e1370)*			199.8	±2.2	10
GC1112 [g]	*daf-16(mu86);daf-2(e1370); naEx148[DAF-16::GFP]*			153.7	±6.8	9
CF1515sib [g, h]	*daf-16(mu86);daf-2(e1370)*			193.6	±6.5	11
CF1515 [g, h]	*daf-16(mu86);daf-2(e1370); muEx212[Pmyo-3::daf-16::GFP]*			174.3	±6.3	28
CF1514sib [g]	*daf-16(mu86);daf-2(e1370)*			192.3	±8.1	10
CF1514 [g]	*daf-16(mu86);daf-2(e1370); muEx211[Pge::daf-16::GFP]*			188.9	±5.6	16
CF1442sib [g]	*daf-16(mu86);daf-2(e1370)*			194.1	±5.4	12
CF1442 [g]	*daf-16(mu86);daf-2(e1370); muEx169[Punc119::daf-16::GFP]*			186.0	±7.1	16
GC1109sib [g]	*daf-16(mu86);daf-2(e1370)*			204.0	±4.6	10
GC1109 [g]	*daf-16(mu86);daf-2(e1370); naEx202 [Plag-2::daf-16::GFP]*			183.3	±3.5	12
GC1144	*daf-16(mu86);daf-2(e1370); naEx202 ; naIs43[Prpl-11.1::daf-16::GFP]*			161.8	±5.5	29
CB1375	*daf-18(e1375)*	L4440		173.2	±6.5	12
CB1375	*daf-18(e1375)*	*ins-1* [c]	*ins-1*	184.5	±10.4	13
CB1375	*daf-18(e1375)*	*ins-3* [c]	*ins-3*	179.8	±8.9	13
CB1375	*daf-18(e1375)*	*ins-33* [c]	*ins-33*	176.9	±7.5	13
RB712	*daf-18(ok480)*	L4440		185.3	±7.3	20
RB712	*daf-18(ok480)*	*ins-1* [c]	*ins-1*	172.1	±7.1	14
RB712	*daf-18(ok480)*	*ins-3* [c]	*ins-3*	179.9	±8.8	16
RB712	*daf-18(ok480)*	*ins-33* [c]	*ins-33*	173.4	±5.2	17
CF1038	*daf-16(mu86)*	L4440		181.3	±6.2	23
CF1038	*daf-16(mu86)*	*ins-1* [c]	*ins-1*	183.2	±5.8	14
CF1038	*daf-16(mu86)*	*ins-3* [c]	*ins-3*	168.7	±3.2	20
CF1038	*daf-16(mu86)*	*ins-33* [c]	*ins-33*	172.6	±4.6	14
CF1038	*daf-16(mu86)*	sjj_C46A5.9 [d]	*hcf-1*	191.9	±6.4	16
CF1038	*daf-16(mu86)*	pGC488 [e]	*daf-2*	194.5	±3.3	15
RB777	*hcf-1(ok559)*			128.4	±9.1	14
GC1071	*ins-3(ok2488)*			162.4	±6.4	18

GC1071	*ins-3(ok2488)*	L4440		168.6	±6.6	15
GC1071	*ins-3(ok2488)*	*ins-3* [c]	*ins-3*	186.5	±2.8	13
GC1071	*ins-3(ok2488)*	*ins-33* [c]	*ins-33*	183.8	±5.1	13
GC1071	*ins-3(ok2488)*	mv_CAA10315 [f]	*daf-18*	218.2	±4.6	11
GC1071	*ins-3(ok2488)*	sjj_R13H8.1 [d]	*daf-16*	216.3	±4.0	15
GC1079sib[g]	*ins-3(ok2488)*			170.8	±6.5	6
GC1079 [g]	*ins-3(ok2488); naEx187[ins3(+)]*			198.6	±4.3	10
GC1088sib[g]				204.3	±5.7	11
GC1088 [g]	*naEx196[ins-3(++)]*			167.5	±5.2	13
GC1039	*ins-33(tm2988)*			170.8	±4.9	20
GC1039	*ins-33(tm2988)*	L4440		166.4	±7.6	15
GC1039	*ins-33(tm2988)*	*ins-3* [c]	*ins-3*	177.6	±4.5	11
GC1039	*ins-33(tm2988)*	*ins-33* [c]	*ins-33*	170.2	±5.4	14
GC1039	*ins-33(tm2988)*	mv_CAA10315 [f]	*daf-18*	204.7	±5.1	16
GC1039	*ins-33(tm2988)*	sjj_R13H8.1 [d]	*daf-16*	214.8	±6.5	16
GC1078sib[g]	*ins-33(tm2988)*			178.6	±4.9	9
GC1078 [g]	*ins-33(tm2988); naEx186[ins-33(+)]*			202.3	±8.0	8
GC1089sib[g]	*ins-33(tm2988)*			168.9	±4.5	11
GC1089 [g]	*ins-33(tm2988); naEx197[ins-33(+)]*			200.6	±6.7	12
GC1087sib[g]	*ins-33(tm2988)*			175.2	±4.8	14
GC1087 [g]	*ins-33(tm2988); naEx195[ins-33(+)]*			198.2	±6.2	12
GC1076sib[g]				214.1	±5.6	10
GC1076 [g]	*naEx184[ins-33(++)]*			204.3	±6.6	12
GC1077sib[g]				219.6	±7.4	9
GC1077 [g]	*naEx185[ins-33(++)]*			217.3	±6.3	9
GC1142	*ins-33(tm2988);ins-3(ok2488)*			183.8	±7.1	16

[a] Worms were grown on OP50 or the indicated RNAi reagent at 20°C from L1 (immediately after hatch-off) until early adulthood, when they were ethanol fixed and DAPI stained. The number of nuclei in the proliferative zone was determined. See Materials and methods (main text) for details.
[b] SEM, standard error of the mean; n, number of gonad arms examined.
[c] RNAi reagent courtesy of Monica Driscoll; see Table S2.
[d] Ahringer library (Kamath et al., 2003).
[e] Vidal library (Rual et al., 2004).
[f] RNAi reagent made for this study; see Table S2.
[g] Sibling progeny from strains bearing transgenes were separated prior to scoring. As indicated under 'Genotype', top line of each pair is data from progeny without the transgene (sibling controls, 'sib') and bottom line of each pair is data from progeny that retained the transgene.
[h] DAF-16::GFP expression in muscle (but not the other tissues) uncovers the 24-hour delay in larval development characteristic of *daf-2(e1370)*, suggesting that *daf-16* activity in the muscle or proximal sheath is important for overall developmental timing.

Table S4. Dauer tests

A

Strain	Genotype	Dauer (%) [a]	*n* [b]
CB1370	*daf-2(e1370)*	0.9	114
DR1309	*daf-16(m26); daf-2(e1370)*	0.0	100

[a] Worms were grown on OP50 at 20°C for 72 hours and scored for the number of dauer worms divided by the total worms on the plate. [Similar results seen for CB1370 in Larsen et al. (Larsen et al., 1995)].
[b] *n*, number of worms examined.
Statistics: *P*>>0.05, one-sided Fisher exact test.

B

Strain	Genotype	Dauer (%) [a]		*n* [b]
CB1370	*daf-2(e1370)*	100.0		100
DR1309	*daf-16(m26); daf-2(e1370)*	0.0		100
CF1442[c]	*daf-16(mu86);daf-2(e1370)*	0.0		100
CF1442[c]	*daf-16(mu86);daf-2(e1370); muEx169[Punc119-daf-16::GFP]*	29.7	*	64

[a] Worms were grown on OP50 at 25°C for 60 hours and scored for the number of dauer worms divided by the total worms on the plate.
[b] *n*, number of worms examined.
[c] Sibling progeny from strains bearing transgenes were separated prior to scoring. As indicated under 'Genotype', top line is data from progeny without the transgene (sibling controls) and bottom line is data from progeny that retained the transgene.
Statistics: *P<0.05, one-sided Fisher exact test versus *daf-2(e1370)* alone or *daf-16(mu86);daf-2(e1370)*; restoration to ~30% dauer is considered rescue (anti-suppression) of *daf-16* (Libina et al., 2003).

C

Strain	Genotype	RNAi	Dauer (%) [a]		*n* [b]
N2		(none)	6.1		49
GC1039	*ins-33 (tm2988)*	(none)	1.2		81
GC1071	*ins-3(ok2488)*	(none)	0.0		65
N2		L4440	12.9		62
N2		*daf-2*	100.0	*	53
N2		*ins-3*	7.2		97
N2		*ins-33*	11.4		79

[a] Worms were grown either on OP50 or on the indicated RNAi (fed on RNAi from parental L4 stage) at 27°C for 60 hours and scored for the number of dauer worms divided by the total worms on the plate. See Table S3 for RNAi reagents.
[b] *n*, number of worms examined.
Statistics: *P<0.05, one-sided Fisher exact test versus L4440 control; for all others, P>> 0.05 (line 2 and 3 versus line 1, and lines 6 and 7 versus line 4).

Table S5. Insulin signaling is not required for normal germ cell size

Strain	Genotype	RNAi reagent	RNAi target	Average volume (μm^3) [a]	SEM[b]	*P*	*n* [b]
FT224		L4440		167.1	±5.1		40
FT224		mv_Y47D3A.16 [c]	*rsks-1*	147.4	±4.2	**	50
FT224		pGC488[d]	*daf-2*	167.2	±4.9		50
FT224		*ins-3* [e]	*ins-3*	173.8	±5.7		40
FT224		*ins-33* [e]	*ins-33*	175.6	±5.8		40
GC1145	*daf-2(e1370)*	none	none	163.9	±4.7		29

[a] SYN-4::GFP-expressing worms were grown on the indicated RNAi reagent from L1 (immediately after hatch-off) until the L4 larval stage, then observed live for GFP fluorescence marking the membranes.
Images were captured in the *z*-plane at 1 μm intervals, and *x*-*y* measurements were taken across two different main axes of the cell (in the *z* plane with the largest cell diameter) using the line measurement tool in Axiovision software (Carl Zeiss). The number of *z* layers was multiplied by the *x* and *y* line measurements to obtain cell volume. For each gonad, five 'cells' were sampled. Note that although germ cells in the proliferative zone are technically syncytial, as they open into a core of shared cytoplasm referred to as the rachis, each nucleus is surrounded by an almost-complete plasma membrane. Therefore it is possible to measure a 'cell' volume despite an opening into the rachis. A total of 8-10 worms were tested for a total of 40-50 individual 'cells' measured.
[b] SEM, standard error of the mean; n, number of cells measured.
[c] Vidal RNAi library (Rual et al., 2004).
[d] RNAi reagent made for this study.
[e] RNAi reagent courtesy of Monica Driscoll.
Statistics: $^{**}P<0.01$, two-tailed Student's *t*-test versus L4440; for others, $P>0.1$.

Table S6. *ins-33* enhances the Pro phenotype of *glp-1(ar202)*

Strain	Genotype	Pro (%) [a]	*n* [b]
GC833	*glp-1(ar202)*	6.5%	214
GC1106	*ins-3(ok2488);glp-1(ar202)*	19.7%	228
GC1009	*ins-33(tm2988);glp-1(ar202)*	29.5%	322

[a] Worms were synchronized by hatch off onto OP50 bacteria and grown to young adulthood at 20°C, then fixed in ethanol, DAPI stained and scored for the Pro phenotype as described (Pepper et al., 2003a; Pepper et al., 2003b).

[b] n, number of worms examined.

Statistics: $P<0.0001$, one-sided Fisher exact test for each double mutant versus the *glp-1(ar202)* single mutant.

Table S7. *ins-3* and *ins-33* ligands are required during stages associated with robust germline proliferation

A

Strain	RNAi	Number of nuclei [a]	SEM [b]	*P*	*n* [b]
N2	L4440	209.5	±7.8		11
N2	*ins-3*	209.4	±4.7		7
N2	*ins-33*	191.8	±8.8		12

B

Strain	RNAi	Number of nuclei [a]	SEM [b]	*P*	*n* [b]
N2	L4440	199.5	±5.4		10
N2	*ins-3*	162.3	±13.0	*	10
N2	*ins-33*	174.6	±7.3	*	10

[a] Parental L4 worms were grown on (A) indicated RNAi reagent/strain or (B) OP50 at 20°C and their progeny were retained on the same bacteria until the mid-L3 stage, at which time they were switched (A) to OP50 or (B) to HT115 bearing the indicated RNAi reagent until adulthood. See Table S1 for RNAi reagents. Worms were grown to the early adult stage, fixed, and DAPI stained (Pepper et al., 2003a). All proliferative zone nuclei were counted.

[b] SEM, standard error of the mean; n, number of gonad arms examined.

Statistics: *$P<0.05$, two-tailed Student's *t*-test versus L4440; for others, $P>0.1$.

Table S8. *daf-16* germline mosaic analysis

Category [a]	Number of animals	% of category	Mother	Brood [b]	Progeny	Interpretation(s) regarding segregation of array	Interpretation(s) regarding role of *daf-16* in brood size
1	20/20	100%	non-Rol	>100	non-Rol, non-GFP	Array absent from maternal soma and germ line.	Large broods in the absence of *daf-16(+)* in any tissues; background value for *daf-16; daf-2*
2A [b]	475/487	97.5%	Rol	10-50 [c]	Rol, GFP [d]	Array present in maternal soma and carried through maternal germ line.	Low brood in the presence of *daf-16(+)* in all tissues including germ line; background value for *daf-16; daf-2*. High correlation of retention of array in germ line with low broods supports hypothesis that *daf-16* is required in germ line downstream of *daf-2*.
2B [b]	11/487	2.3%	Rol	60-80	Rol, GFP [d]	Array present in maternal soma and carried through maternal germ line.	Intermediate brood despite presence of *daf-16(+)* in germ line. Possible loss of array in non-hypodermal lineage in which *daf-16(+)* affects germline proliferation (e.g., EMS) Alternatively, array may not express as well in these individuals, or they may represent a group of individuals that were slightly older when shifted.
2C [b]	1/487	0.2%	Rol	>100	Rol, GFP [d]	Array present in maternal soma and carried through maternal germ line.	Rare class: Large brood size despite presence of *daf-16(+)* in germ line. Either loss of *daf-16* occurred in somatic tissue where *rol-6* is not required and where *daf-16* activity affects germline proliferation. Or array may not be expressed in maternal germ line in this individual.
3 (Mosaic)	12/12	100%	non-Rol	40-60	Rol, GFP [d]	Array not present in somatic focus of *rol-6* activity (including hypodermis lineages, presumed *rol-6* focus) but carried through maternal germ line. Alternatively, error in non-Rol designation of mother (unlikely, see [a]) or *rol-6* not expressed well in hypodermis of individual though present.	Low-intermediate brood with *daf-16(+)* in germ line lineage. Average brood size is somewhat larger than category 2A, suggesting some expression in soma may be responsible for difference.
4A (Mosaic)	17/23	74%	Rol	>100	non-Rol, non-GFP	Array present in maternal soma (particularly hypodermis, presumed focus of *rol-6* activity) and lost in maternal germline. Alternatively, loss of array in P2 since C contributes to hyp7 (a possible focus of *rol-6(+)* activity).	Large brood in animals where *daf-16(+)* is lost from germ line lineage (but not *rol-6*-requiring lineage). Correlation of loss of *daf-16* in germ line with large broods is consistent with requirement for *daf-16* in the germ line

							downstream of *daf-2*. This class may result from loss in P1, which would remove *daf-16* from muscle lineage as well as germ line (see Fig. 3C).
4B (Mosaic)	5/23	22%	Rol	~40	non-Rol, non-GFP	Array present in maternal soma (particularly hypodermis, presumed focus of *rol-6* activity) and lost in maternal germline. Alternatively, loss of array in P2 since C contributes to hyp7 (a possible focus of *rol-6(+)* activity).	Low-intermediate broods from animals where *daf-16(+)* is lost from the germ line lineage. This class may result from loss in P1, which would remove *daf-16* from muscle lineage as well as germ line (see Fig. 3C). Alternatively, loss could have occurred in Z2 or Z3.
4C (Mosaic)	1/23	4%	Rol	~80	non-Rol, non-GFP	Array present in maternal soma (particularly hypodermis, presumed focus of rol-6 activity) and lost in maternal germline. Alternatively, loss of array in P2 since C contributes to hyp7 (a possible focus of *rol-6(+)* activity).	*daf-16(+)* loss from lineage that gives rise to germ line (but not hypodermis) permits large brood. Alternatively, mother may have died prior to producing full brood. Alternatively, loss could have occurred in Z2 or Z3.

[a] Animals of the presumed genotype *daf-16(mu86); daf-2(e1370); muEx108[Pdaf-16::DAF-16::GFP]* were synchronized by hatch-off (Pepper et al., 2003) at 20°C and grown to the early L3 stage. Individual Rol or non-Rol 'mothers' were separated onto individual plates and shifted to 25°C (the Rol phenotype was obvious at this stage in this strain and individuals were subsequently checked as adults). Broods were estimated for each individual starting 48 hours later and continued each day until mother was depleted or dead.

[b] For 30 broods of the 487 in Category 2, exact broods were counted. The average was 23.2±2.7(±SEM) offspring, similar to the average of 17±1.9 observed in *daf-2(e1370)* animals that underwent the same shift protocol. All other brood sizes were estimated by rough counts. Broods '>100' were noticeably different from those designated as '80'.

[c] Animals with broods <10 (253 additional animals) were not included in the analysis as the genotype of the progeny could not be verified.

[d] 'Rol, GFP' indicates that ~15% of the progeny were Rol and GFP+, consistent with the segregation rate of this particular array.